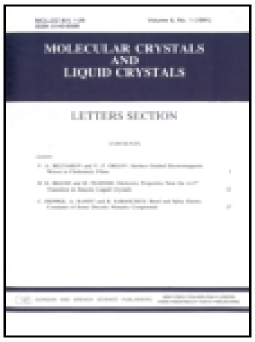

Molecular Crystals and Liquid Crystals

ISSN: 1542-1406 (Print) 1563-5287 (Online) Journal homepage: http://www.tandfonline.com/loi/gmcl20

Synthesis, Characterization, and Structural Investigations of 1-(3-morpholinopropyl)-3-(4-chlorobenzoyl)thiourea monohydrate and 1-(3-morpholinopropyl)-3-(4-methylbenzoyl)thiourea monohydrate

Ibrahim Abdul Razak, Suhana Arshad, Kaliyaperumal Thanigaimani, Mohd Sukeri Mohd Yusof, Sharifah Sakinah Abdullah & Azhar Abdul Rahman

To cite this article: Ibrahim Abdul Razak, Suhana Arshad, Kaliyaperumal Thanigaimani, Mohd Sukeri Mohd Yusof, Sharifah Sakinah Abdullah & Azhar Abdul Rahman (2015) Synthesis, Characterization, and Structural Investigations of 1-(3-morpholinopropyl)-3-(4-chlorobenzoyl)thiourea monohydrate and 1-(3-morpholinopropyl)-3-(4-methylbenzoyl)thiourea monohydrate, Molecular Crystals and Liquid Crystals, 616:1, 151-175, DOI: 10.1080/15421406.2014.990786

To link to this article: http://dx.doi.org/10.1080/15421406.2014.990786

Mol. Cryst. Liq. Cryst., Vol. 616: pp. 151–175, 2015

ISSN: 1542-1406 print/1563-5287 online
DOI: 10.1080/15421406.2014.990786

Synthesis, Characterization, and Structural Investigations of 1-(3-morpholinopropyl)-3-(4-chlorobenzoyl)thiourea monohydrate and 1-(3-morpholinopropyl)-3-(4-methylbenzoyl)thiourea monohydrate

IBRAHIM ABDUL RAZAK,[1,*] SUHANA ARSHAD,[1]
KALIYAPERUMAL THANIGAIMANI,[1] MOHD SUKERI
MOHD YUSOF,[2] SHARIFAH SAKINAH ABDULLAH,[2]
AND AZHAR ABDUL RAHMAN[1]

[1]School of Physics, Universiti Sains Malaysia, USM, Penang, Malaysia
[2]Faculty of Science and Technology, Department of Chemical Sciences,
Universiti Malaysia Terengganu, Mengabang Telipot, Kuala Terengganu,
Malaysia

*Two new compounds, 1-(3-morpholinopropyl)-3-(4-chlorobenzoyl)thiourea monohydrate (**I**) and 1-(3-morpholinopropyl)-3-(4-methylbenzoyl)thiourea monohydrate (**II**) have been synthesized and characterized by FT-IR, ^{1}H NMR, ^{13}C NMR, and Single-Crystal X-Ray Diffraction analyses. Theoretical investigations have been calculated by using DFT method of B3LYP/6-31G + (2d,p) and B3LYP/6-311G + (2d,p) basis sets. Each compound contains a water molecule, forming intra and intermolecular hydrogen bonds with other molecules and further stabilizes the crystal structure. Theoretical calculations of bond parameters, harmonic vibration frequencies, and isotropic chemical shifts are in good agreement with the experimental results. The observed intermolecular interactions in the crystal packing are the main cause of the calculated torsion angles, molecular vibrations, and chemical shifts. The calculated molecular vibrations show good correlation values ranging from 0.995, 0.996, and 0.997 with the experimental data, where the higher basis set fits the experimental results better.*

Keywords Crystal Structure; DFT Studies; Spectroscopy; Thiourea

1. Introduction

Studies on benzoylthiourea derivatives have become one of the interesting subjects due to its potential as neutral ligands. The sulphur, nitrogen, and oxygen donor atoms provide a multitude of bonding possibilities [1, 2]. These compounds are able to coordinate the

---

[*] Address correspondence to Ibrahim Abdul Razak, X-ray Crystallography Unit, School of Physics, Universiti Sains Malaysia 1800, USM, Penang, Malaysia; E-mail: arazaki@usm.my

Color versions of one or more of the figures in the article can be found online at www.tandfonline.com/gmcl.

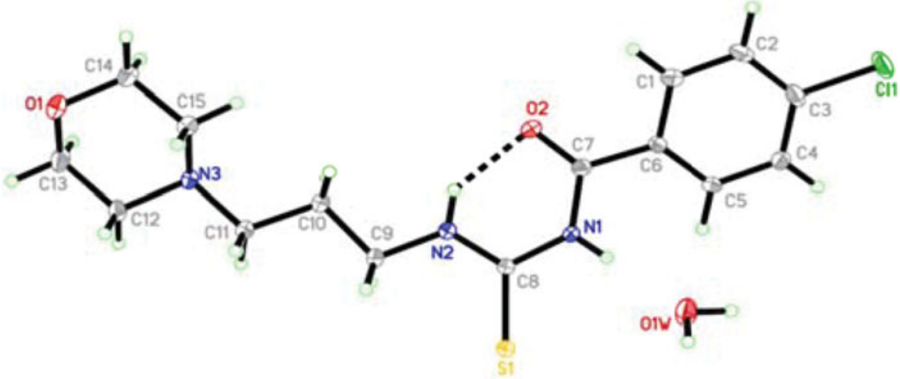

Figure 1. The ORTEP diagram of compound **I** with 50% probability displacement ellipsoid.

metal ion where the ligands typically bond as monoanions through S, N, or O [3, 4] atom. Substituted thiourea derivatives, however, show more diverse coordination chemistry due to their conformational isomerism, steric effects, and presence of donor sites on the substituent groups and intramolecular interactions [5–8]. Thiourea derivatives can be regarded as model compounds for different intra and intermolecular interactions involving S atoms [9, 10]. The coordination chemistry of substituted thioureas has been applied to many interesting fields such as corrosion inhibitor [11–14], agricultural sector [15, 16], pharmaceutical sector [17], catalyst [18–20], and biological sector [21–25].

In the present, computational studies have been widely used because it helps to simulate chemical structures and reactions numerically, based in full or in part on the fundamental law of physics [26]. In order to produce accurate results, choosing the suitable method and the basis set is indeed an important procedure. Studies [2, 27, 28] have shown that the use of DFT (Density Functional Theory)/B3LYP (Becke's three-parameter hybrid method, Lee, Yang and Parr) method is in a good agreement with the observed data compared to the HF (Harthree Fock) method. DFT study includes the effect of electron correlation in the calculation, whereas HF only considers what each electron sees and reacts to an average electron density [26]. In addition, the use of larger basis sets imposes fewer constraints on electrons and more accurately approximate exact molecular orbitals [26].

In continuation of our previous studies [29–32], 1-(3-morpholinopropyl)-3-(4-chlorobenzoyl)thiourea monohydrate and 1-(3-morpholinopropyl)-3-(4-methylbenzoyl) thiourea monohydrate, namely compound **I** and compound **II**, have been synthesized and characterized using FTIR, ^{1}H NMR, and ^{13}C NMR. In order to study their intra- and intermolecular hydrogen bond interactions, the three-dimensional structures of the studied crystal structures were examined by X-Ray crystallography technique. DFT method of B3LYP had been employed to optimize the structure of compounds **I** and **II** at 6-31G + (2d,p) and 6-311G + (2d,p) levels. Herein, we reported the results of geometrical parameters, fundamental frequencies, and GIAO ^{1}H and ^{13}C NMR chemical shift for both basis sets. In combination of the experimental results and quantum chemical calculations, we would like to explore the effect of intra- and intermolecular hydrogen bonds of **I** and **II** at two different basis sets, and to compare predictions made from calculated results with the experimental data that correlates well to which basis set.

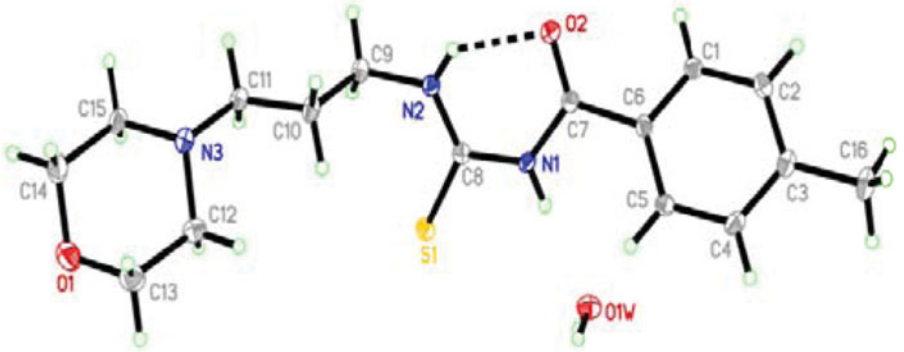

Figure 2. The ORTEP diagram of compound **II** with 50% probability displacement ellipsoid.

2. Results and Discussion

2.1. X-Ray Crystal Structures

The molecular structure of 1-(3-morpholinopropyl)-3-(4-chlorobenzoyl)thiourea monohydrate (**I**) and 1-(3-morpholinopropyl)-3-(4-methylbenzoyl)thiourea monohydrate (**II**) were confirmed by the result of a single crystal X-ray structure diffraction study. Fig. 1 and 2 show the ORTEP diagram of the molecular structure with 50% probability displacement ellipsoids of compounds **I** and **II** respectively. Water molecules (O1W) are trapped in the asymmetric unit of the title compounds, **I** and **II**. The compounds had different para-substituted atoms of the phenyl ring, which were chlorine atom in **I** and methyl group in **II**. The selected bond lengths and angles are listed in Table 1 and the hydrogen bonding parameters are listed in Table 2.

All bond lengths and angles were in the normal range and comparable to the related structures [29–32]. The bond lengths of N1—C7 [1.3762(16) Å for compound **I** and 1.386(2) Å for compound II], N1 C8 [1.3959(16) Å for compound I and 1.393(2) Å for compound **II**] and N2—C8 [1.3246(17) Å for compound **I** and 1.321(2) Å for compound **II**] were shorter than the normal bond length of N—C, which was 1.472 Å. Shorter bond length indicated a partial double bond character along with resonance interactions within the carbonylthiourea group. The same resonance interaction was observed for S–C bond [normal S—C single bond = 1.82 Å and normal S=C double bond = 1.56 Å], where the bond lengths of S1 —C8 for compounds **I** and **II** were 1.6755(14) Å and 1.6880(18) Å, respectively.

Both compounds adopted *trans-cis* configurations with respect to the position of 4-chlorobenzoyl and 4-propylmorpholine for compound **I** and 4-methylbenzoyl and 4-propylmorpholine for compound **II** relative to the S1 atom across their C8-N1 and C8-N2 bonds, which were comparable to the previously reported structures [33,34]. It was found that the intramolecular hydrogen bond between the oxygen atom in the C=O group and the hydrogen atom of the thiourea moiety was favored by the formation of a six-membered ring. In each compound **I** and **II**, an intramolecular N2—H1N2 . . . O2 hydrogen bond was observed with nonbonding distances of N . . . O and the angles of N—H . . . O at 2.6257(15) Å/139.5 (18)° and 2.638(2) Å/135(3)°, respectively. The dashed line in the ORTEP diagram presented in Fig. 1 and Fig. 2 shows the intramolecular hydrogen bond of the compound. The slight differences in bond lengths and angles for both compounds were due to the

Table 1. Selected experimental and calculated geometrical parameters (values in Å and degrees) for compounds **I** and **II**

	Compound **I**			Compound **II**		
Parameters	Experimental	Calculated B3LYP/ 6-31G +(2d,p)	Calculated B3LYP/ 6-311G +(2d,p)	Experimental	Calculated B3LYP/ 6-31G + (2d,p)	Calculated B3LYP/ 6-311G + (2d,p)
			Bond lengths (Å)			
S1−C8	1.6755(14)	1.68929	1.68835	1.6880(18)	1.69321	1.69229
O1−C14	1.4251(16)	1.42038	1.42142	1.427(3)	1.42087	1.42205
O1−C13	1.4305(19)	1.42125	1.42214	1.423(2)	1.42113	1.42233
O2−C7	1.2287(16)	1.23011	1.22811	1.226(2)	1.23084	1.22874
N1−C7	1.3762(16)	1.38120	1.38044	1.386(2)	1.38492	1.38418
N1−C8	1.3959(16)	1.39887	1.39854	1.393(2)	1.39686	1.39623
N1−H1N1	0.85(2)	1.01968	1.01777	0.83(3)	1.01911	1.01763
N2−C8	1.3246(17)	1.33187	1.32914	1.321(2)	1.33287	1.33027
N2−C9	1.4599(16)	1.45694	1.45715	1.460(2)	1.45648	1.45643
N2−H1N2	0.84(2)	1.02116	1.02019	0.82(3)	1.02184	1.02068
N3−C11	1.4705(17)	1.45994	1.46094	1.473(2)	1.46094	1.46100
N3−C15	1.4733(18)	1.46391	1.46381	1.475(2)	1.46285	1.46307
N3−C12	1.4746(16)	1.46361	1.46396	1.473(2)	1.46406	1.46433
O1W−H2W1	0.96(3)	0.98215	0.98181	0.83(3)	0.98183	0.98143
O1W−H1W1	0.87(3)	0.96402	0.96365	0.78(4)	0.96400	0.96358
Cl1−C3	1.7400(13)	1.75094	1.75188			
C3−C16				1.507(2)	1.50809	1.50590
			Bond angles (°)			
C7−N1−C8	126.53(11)	127.74246	127.78300	126.43(15)	127.87931	127.90065
C8−N2−C9	123.37(12)	123.93063	124.13538	123.62(15)	124.95872	124.96240
O2−C7−N1	122.76(12)	122.43199	122.45658	122.69(16)	122.10944	122.20480

O2−C7−C6	121.09(12)	120.79358	120.71921	121.63(15)	121.02706	120.98963
N1−C7−C6	116.15(11)	116.77377	116.82407	115.68(15)	116.86340	116.80549
N2−C8−N1	117.21(12)	116.70699	116.62105	117.65(15)	116.42191	116.38863
N2−C8−S1	123.72(10)	123.52910	123.65554	124.32(13)	124.15898	124.20842
N1−C8−S1	119.07(10)	119.76346	119.72317	118.03(13)	119.41910	119.40294
N2−C9−C10	109.03(11)	110.33815	110.20244	111.53(14)	112.83292	112.88889
C11−C10−C9	110.51(11)	110.95174	111.27462	110.31(14)	111.11647	111.15541
N3−C11−C10	113.34(11)	113.62765	113.38293	114.07(14)	113.58425	113.52865
H2W1−O1W−H1W1	109(2)	105.53993	105.60530	103(3)	105.42664	105.52847
C2−C3−Cl1	119.33(11)	119.38522	119.41016			
C4−C3−Cl1	118.66(11)	119.41127	119.44306			
C2−C3−C16				120.84(17)	120.70659	120.80977
C4−C3−C16				121.22(17)	121.28362	121.17170
			Torsion angles (°)			
C4−C5−C6−C7	176.94(12)	178.68700	178.83211	−177.67(16)	−178.77022	−178.77796
C2−C1−C6−C7	−178.50(12)	−179.24165	−179.28233	178.73(16)	179.27531	179.28552
C8−N1−C7−O2	3.8(2)	3.45658	3.54008	2.3(3)	−3.18633	−3.38259
C8−N1−C7−C6	−175.76(13)	−176.83750	−176.59337	−177.27(15)	176.93010	176.72108
C5−C6−C7−O2	−154.84(13)	−164.01073	−166.99832	144.49(18)	165.79549	166.27404
C1−C6−C7−O2	22.14(19)	14.44255	11.57928	−33.7(2)	−12.83230	−12.39004
C5−C6−C7−N1	24.71(18)	16.27821	13.13267	−35.9(2)	−14.31960	−13.82829
C1−C6−C7−N1	−158.31(12)	−165.26851	−168.28974	145.83(16)	167.05261	167.50763
C9−N2−C8−N1	−176.41(12)	179.03173	179.06395	−176.64(15)	−179.03358	−178.88747
C9−N2−C8−S1	4.1(2)	−0.72359	−0.75483	3.0(2)	0.99088	1.13448
C7−N1−C8−N2	−7.9(2)	−1.10914	−2.32159	−8.6(3)	1.52809	1.77196
C7−N1−C8−S1	171.57(11)	178.65589	177.50472	171.72(14)	−178.49514	−178.24888
C8−N2−C9−C10	175.76(13)	−177.64325	175.74817	77.8(2)	89.29362	89.66319
N2−C9−C10−C11	−171.75(11)	−178.88679	179.75164	−174.16(15)	−179.55090	−179.35508
C15−N3−C11−C10	−62.37(15)	−70.50694	−72.16202	175.92(15)	165.54660	165.21718
C12−N3−C11−C10	177.00(11)	164.98218	163.77132	−64.8(2)	−70.01432	−70.59221
C9−C10−C11−N3	−171.80(11)	−172.33513	−177.07847	176.67(15)	−172.54504	−173.25547
C11−N3−C12−C13	179.32(12)	−177.16143	−177.79692	−174.49(15)	178.36789	178.53316
C1−C2−C3−Cl1	179.54(11)	179.79308	179.80983			
Cl1−C3−C4−C5	179.08(11)	179.77592	179.85530			
C1−C2−C3−C16				179.73(17)	−178.89731	−178.50236
C16−C3−C4−C5				−178.75(17)	179.29960	178.91035

Table 2. Hydrogen bonding distances (Å) and angles (°) in compounds **I** and **II**

Bond D—H... A	Bond length, (Å) D—H	H... A	D... A	Angle D—H... A, (°)
		Compound **I**		
N2—H1N2... O2	0.84(2)	1.929(19)	2.6257(15)	139.5(18)
N1—H1N1... O1W	0.85(2)	2.012(19)	2.8447(16)	168.5(17)
O1W—H2W1... N3 #1[(a)]	0.96(3)	1.87(3)	2.8222(16)	176(2)
O1W—H1W1... S1 #2[(a)]	0.88(3)	2.57(3)	3.4393(12)	172(2)
C4—H4A... S1 #2[(a)]	0.95	2.80	3.4468(15)	126
C15—H15B... O2 #3[(a)]	0.99	2.49	3.4690(16)	169
C14—H14A... *Cg*1[(b)] #4[(a)]	0.99	2.57	3.4828(16)	154
		Compound **II**		
N2—H1N2... O2	0.81(3)	2.01(3)	2.638(2)	135(3)
N1—H1N1... O1W	0.84(3)	2.12(3)	2.955(2)	176(2)
O1W—H1W1... S1 #5[(a)]	0.83(3)	2.57(3)	3.3742(16)	164(3)
O1W—H2W1... N3 #6[(a)]	0.77(4)	2.12(4)	2.888(2)	171(4)
N2—H1N2... O2 #7[(a)]	0.81(3)	2.46(3)	3.050(2)	131(3)
C16—H16B... *Cg*2[(b)] #8[(a)]	0.98	2.76	3.667(2)	155

[a] Symmetry transformations used to generate equivalent atoms: #1 $x-1/2$, $y+1/2$, z; #2 $-x+1/2$, $-y+1/2$, $-z$; #3 $-x+1$, y, $-z+1/2$; #4 $x+1/2$, $-y-1/2$, $z+1/2$; #5 $-x$, $-y+1$, $-z$; #6 x, $y-1$, z; #7 $-x$, $-y+2$, $-z+1$; #8 $-x-1$, $-y+1$, $-z+1$.

[b] *Cg*1 and *Cg*2 are the centroids of the benzene ring for compound **I** and **II**.

different substituents attached to the benzene ring, which contributed to the electron withdrawing effect. Saeed et al. [35] reported that an intramolecular hydrogen bond between the thiourea group and the oxygen atom of the amidic group stabilizes the planar six-membered ring structure. Formation of this (pseudo) ring is important for the molecular conformations because it prevents free rotation within the central carbonyl thiourea moiety and locks its atoms in a nearly planar arrangement [36].

The carbonyl thiourea group (—C(O)NHC(S)NH—) was essentially planar for both compounds **I** [maximum deviation of 0.0756 (11) Å at atom N1] and **II** [maximum deviation of 0.0846 (14) Å at atom O2] where the dihedral angles of O2-C7-N1, N2-C8-S1 and N1-C8-S1 within the carbonylthiourea group were 122.78(12)°, 123.72(10)°, and 119.07(10)° for compound **I** and 122.69(16)°, 124.32(13)°, and 118.03(13)° for compound **II**. In addition, the dihedral angles of C7—N1—C8 were 126.53(11)° (compound **I)** and 126.43(15)° (compound **II)** and C8—N2—C9 were 123.37(12)° (compound **I)** and 123.62(15)° (compound **II)** where these angles show a sp^2 hybridization on the N1 and N2 atoms. The benzene rings (C1/C2/C3/C4/C5/C6) were essential planar with maximum deviations of 0.010(1) Å at atom C1 and 0.009(2) Å at atom C4, respectively to compound **I** and compound **II**. Meanwhile, the morpholine ring (O1/N3/C12/C13/C14/C15) in both compounds adopted chair conformations [37] with puckering parameters of $Q = 0.5799\ (14)$ Å, $\Theta = 178.46(15)°$, and $\Phi = 74(5)°$ for compound **I** and $Q = 0.573\ (2)$ Å, $\Theta = 178.61\ (19)°$, and $\Phi = 202\ (10)°$ for compound **II**. The same ring conformations were also reported in the related compounds that consisted of morpholine ring moiety [38–40]. In compound **I,** the whole molecule was almost planar except at the terminal chloro-substituted benzene ring where it

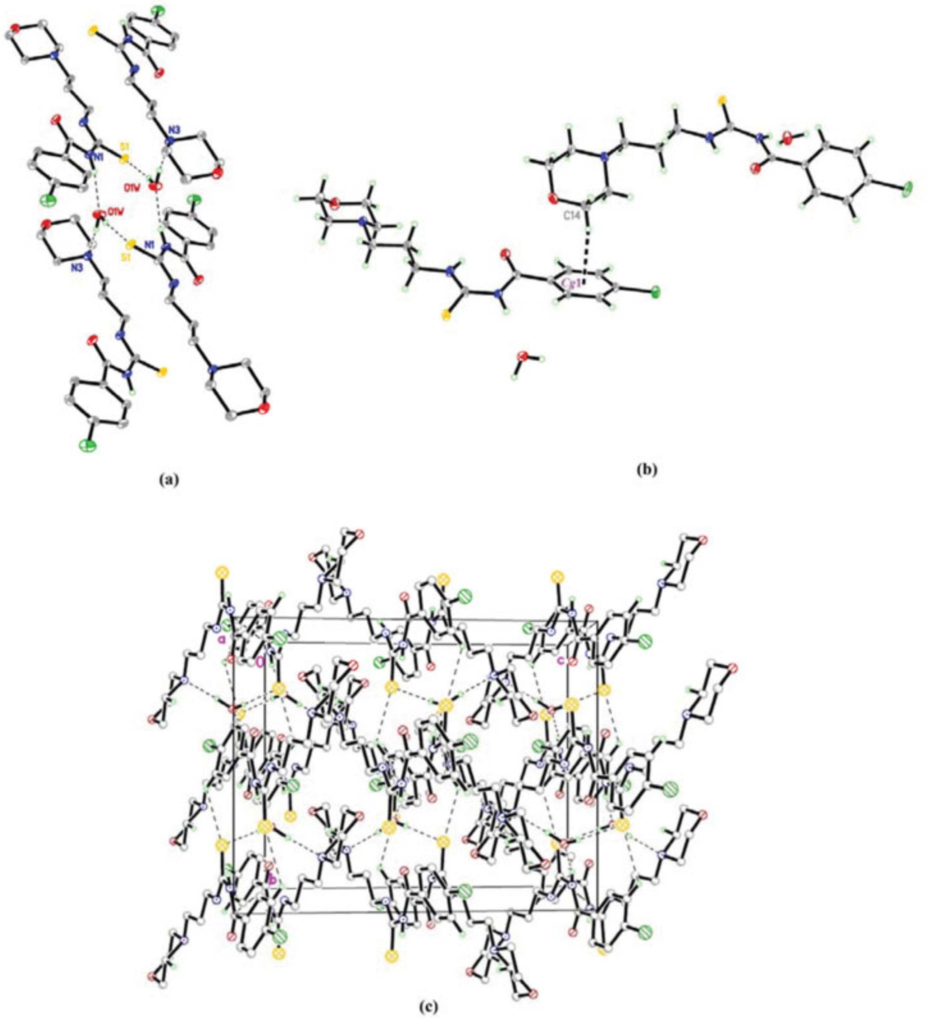

Figure 3. Hydrogen bonding interactions in Compound **I:** (a). Interaction with the water solvent; (b). C—H . . . π interaction; (c). The crystal packing of the compound connected into a three-dimensional network.

slightly twisted at C6—C7 bond with the C1—C6—C7—N1 torsion angle of −158.31(12)°. In compound **II**, the methyl-substituted benzene ring (C1/C2/C3/C4/C5/C6/C16) and the 4-propylmorpholine ring (O1/N3/C9/C10/C11/C12/C13/C14/C15) were twisted away from the carbonylthiourea moiety (—C(O)NHC(S)NH—) at C6—C7 bond [C1—C6—C7—N1 torsion angle of 145.83(16)°] and C9—C10 bond [C8—N2—C9—C10 torsion angle of 77.8(2)°].

The crystal structure of compounds **I** and **II** is shown in the Figs 3 and 4, respectively. Figures 3(a) and 4(a) show the intermolecular hydrogen interactions between the main molecules with the water molecules. The same intermolecular N1—H1N1 . . . O1W, O1W—H2W1 . . . N3, and O1W—H1W1 . . . S1 hydrogen bonds (Table 2) were involved between the molecules and water solvents in both compounds but displayed different types

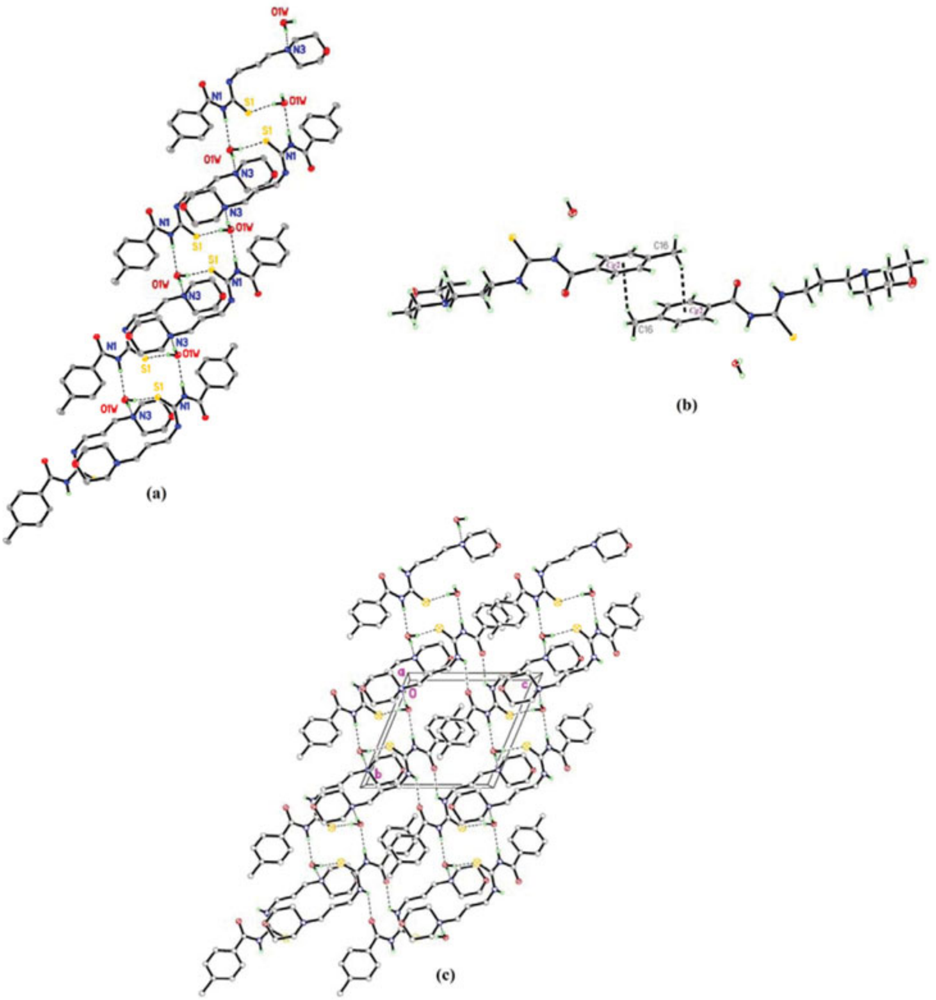

Figure 4. Hydrogen bonding interactions in Compound **II:** (a). Interaction with the water solvent; (b). C—H . . . π interaction; (c). The crystal packing of the compound connected into a three-dimensional network.

of crystal packing arrangement. In compound **I**, the molecules were linked into a centrosymmetric dimer and generate R_4^4 (12) ring motif [41]. Meanwhile in compound **II,** the intermolecular interaction between water molecules and the sulphur atoms formed R_4^4 (12) ring motifs [41] and further connected into infinite one-dimensional column by intermolecular O1W—H2W1 . . . N3 hydrogen bonds (Table 2). The molecules in compound **I** were connected into a three-dimensional network as shown in Fig. 3(c) by C4—H4A . . . S1 and C15—H15B . . . O2 hydrogen bonds (Table 2) and stabilized by C—H . . . π interactions, generated by symmetry transformation of $x+1/2$, $-y-1/2$, $z+1/2$ where π ($Cg1$) was the centroid of the terminal benzene ring (C1/C2/C3/C4/C5/C6), Fig. 3(b). Different crystal packing was formed by molecules in compound **II**, which is shown in Fig. 4(a)–(c). Intermolecular N2—H1N2 . . . O2 hydrogen bonds (Table 2) connected the molecules into a two-dimensional sheet parallel to *bc*-axis. These intermolecular

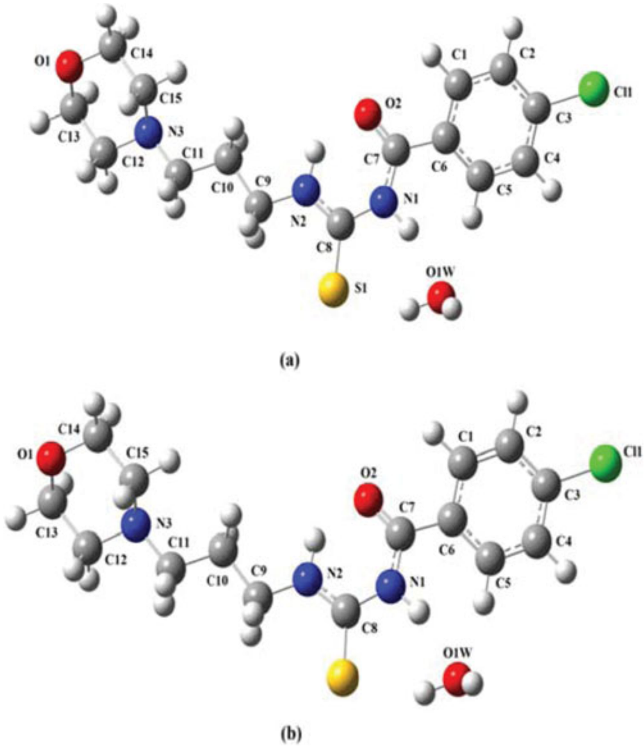

Figure 5. Optimized structure of Compound **I** at (a) DFT B3LYP/6-31G+(2d,p); (b) DFT B3LYP/6-311G+(2d,p).

N—H... O hydrogen bonds further formed $R_2{}^2$ (12) graph-set motifs [41]. C—H... π interactions (symmetry code: $-x-1$, $-y+1$, $-z+1$) involving the centroid of the benzene ring ($Cg2$ = C1/C2/C3/C4/C5/C6) were also observed. The carbonyl thiourea group (—C(O)NHC(S)NH—) and the nitrogen atom within the morpholine ring played an important role in generating supramolecular hydrogen bond with the water molecules. In addition, the carbonyl thiourea moieties which contained three potential donor atoms (N, O, and S) became the utility among organic reagents as potential donor ligands for transition metal ions.

The molecular structures obtained from X-Ray crystallography analysis were performed a full geometry optimization for the purpose of theoretical and experimental data comparison. The structures were calculated by DFT method with two different basis sets of B3LYP/6-31G+(2d,p) and B3LYP/6-311G+(2d,p). Fig. 5 and Fig. 6 show the optimized structures of both compounds and Table 1 lists out the selected bond lengths and angles of the optimized structures where the calculated bond lengths and angles were in a good agreement with the experimental results. The calculated bond lengths and angles for basis set of B3LYP/6-311G+(2d,p) indicated the best agreement with the experimental values in both compounds.

The optimized structures for basis set of B3LYP/6-31G+ (2d,p) and B3LYP/6-311G+ (2d,p) for compound **I** is shown in Fig. 5(a) and (b), respectively. The bond lengths for N1—C7 [1.38120 and 1.38044 Å], N1—C8 [1.39887 and 1.39854 Å], and N2—C8 [1.33187 and 1.32914 Å] were in a good agreement with the X-ray diffraction results indicating that

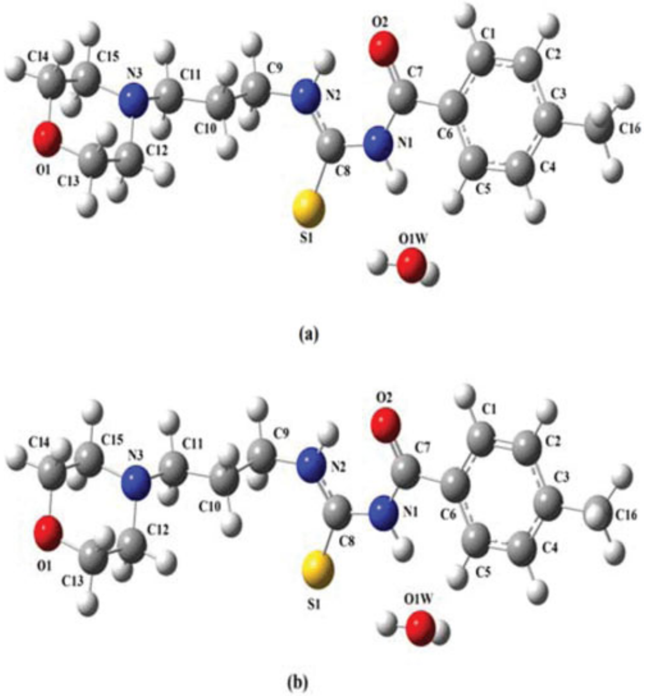

Figure 6. Optimized structure of Compound **II** at (a) DFT B3LYP/6-31G+(2d,p); (b) DFT B3LYP/6-311G+(2d,p).

the partial double bond character existed within the optimized thiourea moiety. These bond characters were the results of the intramolecular N—H... O hydrogen bond that locked the molecule to form a six-membered ring motif. In addition, the similar trend of C—N bond lengths has been obtained from these species [N2—C8<N1—C7<N1—C8] and this trend also reproduced by the quantum chemical calculations suggesting intramolecular are responsible for the observed N—C bond lengths values rather than the crystal packing effects [7,35,42]. However, compound **II** showed the same bond length values for N1–C7 [1.38492 and 1.38418 Å], N1—C8 [1.39686 and 1.39623 Å], and N2—C8 [1.33287 and 1.33027 Å] but the observed simulated bond length of N1—C7 shown in Fig. 6(a) and (b) possessed a single bond criteria. The different substituent atom attached to the benzene ring may have affected the criteria of the optimized C–N bond length, where the substituted-methyl group (compound **II**) was the electron donating group as compared to the substituted-chlorine atom (compound **I**), which was the electron withdrawing group. Various electron-donating or -withdrawing substituents affected the hydrogen-bonding ability of the thiourea, which depended on the acidity of the thioureido —NH protons that provided additional bonding site [35].

From Table 1, the nonhydrogen bonding atoms provide a good result with the experimental data compared to the hydrogen-attached atoms; examples in this compound are N–H and O—H bonds. The calculated N—H bond lengths in both compounds for both basis sets showed higher values than the experimental results [0.82 to 0.85 Å], where the values varied between 1.01763 to 1.02116 Å. The bond angles of the water molecules (H2W1—O1W—H1W1) were slightly different from the experimental results, where the angle differences ranged between 2 to 4°. The differences between the experimental and theoretical values were due to the environment factor where the theoretical calculations were performed in gaseous state, whereas the experimental data belonged to the solid phase.

From the optimized structure of **I**, the dihedral angle between the carbonyl thiourea ring made up by the intramolecular N2—H1N2 . . . O2 and the benzene ring is shown by the torsion angle C1—C6—C7—O2 value of 14.44255° [B3LYP/6-31G+(2d,p)] and 11.57928° [B3LYP/6-311G+(2d,p)]. The corresponding torsion angle values in **II** are −12.83230° [B3LYP/6-31G+(2d,p)] and −12.39004° [B3LYP/6-311G+(2d,p)]. The differences between this values compared to the corresponding experimental values [Table 1] are due to the intermolecular C15—H15B . . . $O2^{\#3}$ (compound **I**) and N2—H1N2 . . . $O2^{\#7}$ (compound **II**) interactions affecting the molecular structure and the intramolecular N—H . . . O hydrogen bond interaction [6]. The significant difference between the experimental and theoretical values can also be seen with the C15—N3—C11—C10 and C8—N2—C9—C10 torsion angles of compound **II** which are due to O1W—H2W1 . . . N3 and N2—H1N2 . . . O2 intermolecular hydrogen bonds (symmetry code in Table 2), respectively.

2.2. Vibrational Analysis

The harmonic vibrational frequencies calculated at DFT level with the diffused and polarization functions, B3LYP/6-31+(2d,p) and B3LYP/6-311G+(2d,p) along with the experimental frequencies, relative intensities and probable assignments are summarized in Tables 3 and 4. The experimental and calculated FT-IR spectra for both compounds are shown in Fig. 7. The calculated frequencies were performed for a free molecule in vacuum, while the experimental frequencies are in the solid state. Comparison of the calculated and the experimental frequencies revealed the overestimation of the calculated wavenumbers corresponding to observed results because of the combination of electron correlation effects and basis set deficiencies. Furthermore, the slight disagreement between theory and experiment could be due to neglect of the anharmonicity in the real system. Therefore, in order to improve the agreement with the experiment data, it is customary to scale down the calculated harmonic wavenumbers. In our study, we have used a scaling factor of 0.9613 and the vibrational wavenumbers suited well with experimental data.

The stretching frequencies of O—H bonds of the water molecule can be observed at 3487.61 and 3467.70 cm^{-1} in compounds **I** and **II**, respectively. Meanwhile, the stretching N—H group was clearly observed in the range of 3100 cm^{-1} to 3400 cm^{-1}. The calculated frequencies of B3LYP/6-31G+(2d,p) and B3LYP/6-311G+(2d,p) gave the values of wavenumbers at 3365.51 (O—H)/3284.28 (N—H) cm^{-1} and 3365.41 (O—H)/3274.21 (N—H) cm^{-1} in compound **I**, respectively. Meanwhile, the corresponding values were 3373.57 (O-H)/3268.95 (N—H) cm^{-1} for B3LYP/6-31G+(2d,p) and 3372.51 (O—H) /3262.85 cm^{-1} (N—H) for compound **II**. These assignments were due to the formation of intra- and intermolecular hydrogen bonds formed by the N—H and O—H bonds.

The strong carbonyl bands were clearly observed at 1666.63 and 1663.09 cm^{-1} in compounds **I** and **II**, respectively. These values were decreasing compared to the vibration of carbonyl group (1710 cm^{-1}). Meanwhile, the calculated carbonyl frequencies were 1643.02 cm^{-1} [B3LYP/6-31G+(2d,p)] and 1634.85 cm^{-1} [B3LYP/6-311G+(2d,p)] for compound **I** and 1614.77 cm^{-1} [B3LYP/6-31G+(2d,p)] and 1633.71 cm^{-1} [B3LYP/6-311G+(2d,p)] for compound **II**. Perhaps the strong C=O stretching bands were related to the effect of conjugated resonance with the phenyl ring and the formation of intramolecular N—H . . . O hydrogen bond within the molecules.

Table 3. Comparison of the theoretical and experimental vibrational spectra and proposal assignment for compound **I**

	Calculated IR (km mol^{-1})						
Experimental	B3LYP 6-31G + (2d,p)			B3LYP 6-311G + (2d,p)			
(cm^{-1})	Unscaled	Scaled	IR$_{int}$	Unscaled	Scaled	IR$_{int}$	Assignments $^{(a)}$
	3862.41	3712.935	85.73	3860.84	3711.425	81.14	ν_{as}OH
3487.61	3501.00	3365.511	799.43	3500.90	3365.415	814.08	ν_sOH, ν_sNH
	3427.89	3295.231	179.51	3434.17	3301.268	111.85	ν_sOH, ν_sNH
3161.84	3416.50	3284.281	195.86	3406.02	3274.207	249.22	ν_sOH, ν_sNH
	3221.51	3096.838	2.86	3209.27	3085.071	2.74	ν_sCH
	3216.87	3092.377	2.35	3203.24	3079.275	2.38	ν_sCH
	3207.75	3083.610	0.53	3196.05	3072.363	0.41	ν_{as}CH
3034.64	3201.37	3077.477	4.61	3186.60	3063.279	7.50	ν_{as}CH
	3098.22	2978.319	26.20	3091.17	2971.542	23.78	ν_{as}CH$_2$
2961.22	3097.22	2977.358	44.98	3089.52	2969.956	45.31	ν_{as}CH$_2$
2939.85	3087.37	2967.889	37.64	3080.19	2960.987	39.26	ν_{as}CH$_2$
	3077.72	2958.612	31.70	3070.52	2951.691	30.48	ν_{as}CH$_2$
	3060.80	2942.347	35.73	3053.66	2935.483	29.33	ν_{as}CH$_2$
	3058.27	2939.915	2.42	3051.60	2933.503	7.37	ν_{as}CH$_2$
	3046.53	2928.629	17.50	3040.17	2922.515	13.11	ν_{as}CH$_2$
	3034.55	2917.113	13.16	3030.97	2913.671	11.77	ν_sCH$_2$
2876.24	3028.20	2911.009	2.51	3022.57	2905.597	4.43	ν_sCH$_2$
2854.63	2987.24	2871.634	94.48	2984.83	2869.317	92.00	ν_sCH$_2$
	2982.64	2867.212	22.12	2980.70	2865.347	19.99	ν_sCH$_2$
2829.49	2917.83	2804.910	140.82	2916.24	2803.382	129.70	ν_sCH$_2$
2778.82	2906.69	2794.201	36.90	2904.16	2791.769	40.47	ν_sCH$_2$
	2898.93	2786.741	34.84	2898.95	2786.761	28.50	ν_sCH$_2$
1666.63	1709.16	1643.016	181.50	1700.66	1634.844	173.67	ν CO, δNH
	1648.39	1584.597	19.43	1648.18	1584.395	16.14	δOH, δNH
	1634.93	1571.658	106.89	1631.92	1568.765	110.74	ν CC, δNH
1592.25	1609.13	1546.857	214.33	1603.66	1541.598	197.58	ν CC, ν CN, δOH, δNH
1559.04	1604.81	1542.704	215.74	1600.15	1538.224	249.76	ν CC, ν CN, δOH, δNH
1528.24	1580.06	1518.912	851.41	1578.22	1517.143	811.71	ρ CN, δNH
1486.87	1525.39	1466.357	62.12	1528.71	1469.549	78.09	ν CC, ρCH, δNH
1404.02	1517.82	1459.080	17.87	1507.98	1449.621	19.68	δCH$_2$
	1505.84	1447.564	11.32	1500.14	1442.085	12.70	δCH$_2$
	1498.02	1440.047	14.20	1496.98	1439.047	8.28	δCH$_2$
	1494.67	1436.826	8.71	1491.57	1433.846	9.60	δCH$_2$
	1488.77	1431.155	10.17	1487.30	1429.741	1.08	δCH$_2$
	1483.61	1426.194	0.58	1483.07	1425.675	0.33	δCH$_2$
	1479.34	1422.090	0.54	1436.64	1381.042	5.32	δCH$_2$
	1437.47	1381.840	17.93	1435.27	1379.725	29.53	ωCH$_2$
	1433.52	1378.043	23.58	1420.00	1365.046	3.53	ρCH, ωCH$_2$, ν CN
	1416.92	1362.085	12.13	1413.37	1358.673	11.52	ωCH$_2$, ν CN, δNH
	1416.12	1361.316	5.29	1404.14	1349.800	30.73	ωCH$_2$, ν CN, δNH
1378.08	1405.77	1351.367	35.36	1389.20	1335.438	49.81	ωCH$_2$, ν CN, δNH
1360.74	1388.31	1334.582	57.98	1370.42	1317.385	114.30	ωCH$_2$, ν CN, δNH
1307.68	1373.50	1320.346	94.83	1365.84	1312.982	8.83	ωCH$_2$, ν CN, δNH, ν CS
	1364.59	1311.780	0.84	1346.01	1293.919	17.51	ωCH$_2$
	1342.20	1290.257	11.80	1340.98	1289.084	12.94	tCH$_2$
	1340.26	1288.392	8.40	1335.30	1283.624	3.70	ν CC,ρCH
	1338.35	1286.556	28.91	1322.75	1271.560	10.62	ν CC,ρCH, ν CN, δNH
	1333.81	1282.192	5.30	1320.61	1269.502	28.12	tCH$_2$
	1320.60	1269.493	9.15	1308.70	1258.053	17.65	tCH$_2$
	1308.82	1258.169	21.49	1302.25	1251.853	14.02	tCH$_2$, ωCH$_2$
1292.14	1302.77	1252.353	13.89	1286.92	1237.116	16.12	tCH$_2$
1265.92	1289.97	1240.048	366.72	1281.06	1231.483	415.14	ν CN, δNH, ν CC
1212.18	1243.58	1195.453	1.26	1244.27	1196.117	1.93	tCH$_2$, ωCH$_2$
	1232.94	1185.225	3.22	1233.80	1186.052	2.26	tCH$_2$
	1217.94	1170.806	36.90	1219.06	1171.882	25.59	ρCH
1175.88	1206.22	1159.539	166.10	1195.22	1148.965	154.31	ν CN, δNH

Table 3. Comparison of the theoretical and experimental vibrational spectra and proposal assignment for compound **I** (*Continued*)

	Calculated IR (km mol^{-1})						
Experimental	B3LYP 6-31G+(2d,p)			B3LYP 6-311G+(2d,p)			
(cm^{-1})	Unscaled	Scaled	IR$_{\text{int}}$	Unscaled	Scaled	IR$_{\text{int}}$	Assignments $^{(a)}$
1146.96	1193.95	1147.744	43.71	1189.58	1143.543	97.66	ν CN, δNH, *t*CH$_2$
	1169.42	1124.163	56.34	1164.27	1119.213	29.07	ν CN, ρCH
	1153.92	1109.263	14.83	1151.65	1107.081	29.58	ν CN, ρCH, δCH$_2$
	1140.49	1096.353	12.65	1141.02	1096.863	25.48	ρCH
	1135.62	1091.672	28.31	1132.49	1088.663	42.76	ν CN, ν CC, ρCH
1115.09	1133.71	1089.835	96.57	1130.36	1086.615	70.33	ν CN, ν CC, ν CO
	1115.30	1072.138	4.36	1112.18	1069.139	9.99	ωCH$_2$
1091.63	1109.26	1066.332	99.53	1106.86	1064.025	112.34	ν CN, ν CC, ν CCl
1071.47	1096.98	1054.527	14.85	1092.40	1050.124	14.61	ν CN, ν CC, ν CCl
1052.30	1093.10	1050.797	7.54	1092.02	1049.759	4.91	ρCH$_2$
1040.93	1062.88	1021.747	12.86	1059.42	1018.420	15.42	ν CC, ν CS, ν CN
1010.53	1051.71	1011.009	15.61	1048.58	1008.000	18.14	ν CC, ν CS
	1043.98	1003.578	2.23	1039.86	999.6174	1.32	ν CC, ν CO, ν CN
	1027.93	988.1491	44.93	1033.20	993.2152	45.37	ν CC, ρCH
	1016.76	977.4114	26.42	1012.96	973.7584	29.77	ν CC, ν CO, ν CN
917.96	995.51	956.9838	1.27	997.07	958.4834	0.63	*t*CH
900.18	990.40	952.0715	0.27	991.87	953.4846	0.21	*t*CH
880.98	927.28	891.3943	7.24	925.52	889.7024	6.55	ν CC, ν CO, ν CN, ρCH$_2$
861.71	911.92	876.6287	35.02	912.19	876.8882	30.41	ν CC, ν CN
850.87	883.53	849.3374	18.26	885.16	850.9043	15.52	ρCH$_2$, *t*CH$_2$
	871.89	838.1479	31.02	870.73	837.0327	34.83	ρCH$_2$, ωCH
	871.06	837.3500	12.09	870.23	836.5521	11.40	ρCH$_2$, ωCH
	861.54	828.1984	0.82	860.75	827.4390	0.93	ρCH$_2$
	849.95	817.0569	1.19	846.81	814.0385	1.01	ωCH
788.60	810.37	779.0087	11.82	808.08	776.8073	10.69	ν CC, ν CO, ν CN, ν CS
764.76	795.54	764.7526	43.99	794.30	763.5606	44.78	ν CS, ν CC
	777.49	747.4011	67.10	777.02	746.9493	65.20	ωCH
	762.60	733.0874	1.13	762.90	733.3758	1.83	ρCH$_2$
	737.88	709.3240	48.99	732.14	703.8062	61.94	ωNH
709.24	725.55	697.4712	4.29	726.75	698.6248	5.73	ν CCl, ν CC, ν CS
	698.02	671.0066	2.03	697.13	670.1511	1.41	*t*OH
626.21	662.93	637.2746	255.08	659.22	633.7082	246.94	ν CC
	641.54	616.7124	1.52	645.45	620.4711	1.85	ωCH$_2$, ωCS
	636.46	611.8290	17.02	637.19	612.5307	16.87	ωCH$_2$, ωCS
	635.57	610.9734	2.79	634.85	610.2813	5.64	ρCS, ωCH$_2$
548.81	609.95	586.3449	1.28	609.52	585.9316	1.35	ν CC, ν CCl
	546.69	525.5331	32.35	545.91	524.7833	31.81	ν CC, ν CO, ν CN
489.62	499.56	480.2270	4.73	497.74	478.4775	2.79	ν CC, ν CO, ν CN, ν CCl
477.23	497.68	478.4198	2.97	497.12	477.8815	5.28	ω CC, ωCN, ωCS, ωCO
	490.98	471.9791	7.85	491.78	472.7481	5.85	ω CC, ωCN, ωCS, ωCO
	468.57	450.4363	2.73	466.95	448.8790	2.76	ω CC, ωCN, ωCS, ωCO
418.64	431.50	414.8010	1.31	431.26	414.5702	1.65	ρCC, ρCN, ρCCl, ρCO
	418.79	402.5828	0.37	419.22	402.9962	0.48	*t*CH
	416.85	400.7179	0.87	414.06	398.0359	0.80	ρCH$_2$, ρCC
	375.66	361.1220	4.40	377.81	363.1888	4.59	ρCO, ν CN, ν CS, δNH
	355.35	341.5980	60.01	362.24	348.2213	63.00	ρOH
	341.36	328.1494	21.12	342.27	329.0242	20.75	ρCC, ρCN, ρCCl, ρCO, ρCS
	333.73	320.8146	7.59	333.55	320.6416	6.83	ρCH$_2$
	309.41	297.4358	9.42	309.81	297.8204	10.24	ωCH$_2$
	291.06	279.7960	5.43	290.52	279.2769	5.08	*t*CC, *t*CN
	278.57	267.7893	20.87	277.46	266.7223	4.54	*t*CC, *t*CN, ω OH
	274.10	263.4923	78.52	269.82	259.3780	96.58	*t*CC, *t*CN, ω OH
	256.41	246.4869	0.72	256.11	246.1985	0.80	ρCH$_2$
	233.27	224.2425	3.78	234.16	225.0980	4.20	ρCC, ρCCl, ρCS
	220.80	212.2550	6.61	218.32	209.8710	6.61	ρCH$_2$, ρOH
	201.82	194.0096	0.63	202.09	194.2691	0.22	ρCH$_2$, ρCS

Table 3. Comparison of the theoretical and experimental vibrational spectra and proposal assignment for compound **I** (*Continued*)

Experimental	Calculated IR (km mol^{-1})						
	B3LYP 6-31G+(2d,p)			B3LYP 6-311G+(2d,p)			
(cm^{-1})	Unscaled	Scaled	IR$_{\text{int}}$	Unscaled	Scaled	IR$_{\text{int}}$	Assignments $^{(a)}$
	175.70	168.9004	8.66	175.17	168.3909	8.65	Skeletal vibration
	137.97	132.6306	8.22	138.37	133.0151	8.09	Skeletal vibration
	130.64	125.5842	1.81	132.04	126.9301	1.88	Skeletal vibration
	129.37	124.3634	0.34	129.56	124.5460	0.33	Skeletal vibration
	110.89	106.5986	0.08	112.47	108.1174	0.61	Skeletal vibration
	109.57	105.3296	4.15	107.81	103.6378	3.77	Skeletal vibration
	89.16	85.70951	0.28	85.31	82.00850	0.19	Skeletal vibration
	82.89	79.68216	0.52	77.27	74.27965	0.60	Skeletal vibration
	74.21	71.33807	0.72	75.22	72.30899	0.84	Skeletal vibration
	48.69	46.80570	1.86	48.15	46.28660	1.65	Skeletal vibration
	36.41	35.00093	0.15	35.51	34.13576	0.11	Skeletal vibration
	32.59	31.32877	0.10	33.21	31.92477	0.19	Skeletal vibration
	24.51	23.56146	0.03	24.50	23.55185	0.01	Skeletal vibration
	21.48	20.64872	0.04	17.07	16.40939	0.03	Skeletal vibration
	14.53	13.96769	0.14	11.05	10.62237	0.20	Skeletal vibration

[a] Vibrational assignment: ν, stretching; δ, scissoring; ω, wagging; ρ, rocking; t, twisting.

The C—N vibration bands were observed at 1551, 1265, and 1171 cm^{-1}, respectively, to $\delta_{\text{CN-H}}$, $\nu_{\text{C(O)-N}}$, and $\nu_{\text{C(S)-N}}$ as reported in the related structure of thiourea [33]. The same vibrational bands of $\delta_{\text{CN-H}}/\nu_{\text{C(O)-N}}/\nu_{\text{C(S)-N}}$ at 1528.24/1265.92/1175.88 cm^{-1} and 1554.37/1261.08/1174.80 cm^{-1} can be clearly seen in compounds **I** and **II**, respectively. The wavenumbers of 1528.24 and 1554.37 cm^{-1} showed the bending vibration of CN—H and revealed the existence of intramolecular N—H... O hydrogen bond. Meanwhile, the determinations of the other two vibrational bands were by the help of DFT method calculations, where the stretching C—N vibrations were assigned within the same range with the experimental values. The calculated bending and stretching C—N bands appeared at 1518.91/1240.05/1159.54 cm^{-1} [B3LYP/6-31G+(2d,p)] and 1517.14/1231.48/1148.97 cm^{-1} [B3LYP/6-311G+(2d,p)] for compound **I**, whereas in compound **II** the values were 1528.31/1240.69/1137.82 cm^{-1} [B3LYP/6-31G+(2d,p)] and 1527.24/1232.87/1131.38 cm^{-1} [B3LYP/6-311G+(2d,p)]. The high value of C—N absorption observed in the experimental and theoretical analysis maybe related to δ(C—H) contribution from the substituent group [5]. The lower vibration frequency of νC—N, which normally is around 1300 cm^{-1} could be due to the mass effect around the nitrogen atom [43].

The IR absorptions of C=S band were observed at 764.76 and 756.76 cm^{-1} for compounds **I** and **II**, respectively and the values were in a good agreement with the calculated values. The calculated B3LYP/6-31G+(2d,p)/B3LYP/6-311G+(2d,p) showed the values of 679.47/698.62 cm^{-1} and 731.62/720.35 cm^{-1}, respectively. The formation of the intermolecular hydrogen bond interactions between the water molecule and the sulphur atoms may have affected the values ν(C=S), where the presence of intermolecular hydrogen bonds were confirmed by the X-Ray analysis.

The frequency values computed at B3LYP/6-31G+(2d,p) and B3LYP/6-311G+(2d,p) level contained known systematic error. By plotting the calculated values against experimental frequency, linearity between the experimental and calculated vibrational frequency can be determined, which has been presented in Fig. 8. Different basis sets somehow would

Table 4. Comparison of the theoretical and experimental vibrational spectra and proposal assignment for compound **II**

	Calculated IR (km mol^{-1})						
Experimental	B3LYP 6-31G+(2d,p)			B3LYP 6-311G+(2d,p)			
(cm^{-1})	Unscaled	Scaled	IR$_{\mathrm{int}}$	Unscaled	Scaled	IR$_{\mathrm{int}}$	Assignments$^{(a)}$
	3863.29	3713.7807	85.69	3862.38	3712.9059	81.20	ν_{as}OH
3467.70	3509.38	3373.5670	786.01	3508.28	3372.5096	795.66	ν_sOH, ν_sNH
	3440.84	3307.6795	102.15	3440.28	3307.1412	92.67	ν_sOH, ν_sNH
3436.19	3400.55	3268.9487	338.59	3394.20	3262.8445	337.55	ν_sNH
	3214.24	3089.8489	3.03	3202.24	3078.3133	2.86	ν_sCH
	3208.77	3084.5906	5.06	3195.46	3071.7957	5.82	ν_sCH
	3176.42	3053.4925	12.19	3164.95	3042.4664	11.05	ν_{as}CH
	3172.10	3049.3397	15.10	3161.69	3039.3326	13.98	ν_{as}CH
3144.83	3114.82	2994.2765	13.70	3104.59	2984.4424	12.72	$\nu_a CH_3$
	3111.48	2991.0657	17.30	3101.99	2981.9430	15.83	$\nu_{as} CH_2$
	3098.77	2978.8476	26.50	3090.78	2971.1668	24.90	$\nu_s CH_2$
2957.67	3095.97	2976.1560	46.11	3088.11	2968.6001	44.77	$\nu_{as} CH_2$
2940.02	3093.48	2973.7623	12.97	3084.40	2965.0337	17.30	$\nu_{as} CH_2$
	3084.72	2965.3413	12.86	3076.25	2957.1991	15.18	$\nu_{as} CH_3$
	3081.30	2962.0537	19.53	3073.38	2954.4402	16.16	$\nu_{as} CH_2$
2857.98	3056.51	2938.2231	43.45	3050.12	2932.0804	42.02	$\nu_{as} CH_2$
	3048.24	2930.2731	40.70	3043.88	2926.0818	37.12	$\nu_s CH_2$
	3041.44	2923.7363	11.23	3036.16	2918.6606	10.20	$\nu_s CH_2$
	3033.77	2916.3631	13.77	3029.02	2911.7969	13.05	$\nu_{as} CH_2$
	3029.20	2911.9700	27.24	3024.33	2907.2884	22.49	$\nu_s CH_3$
	2986.28	2870.7110	95.62	2983.73	2868.2596	93.10	$\nu_s CH_2$
	2981.66	2866.2698	23.59	2979.51	2864.2030	21.63	$\nu_s CH_2$
2829.28	2918.76	2805.8040	134.37	2916.48	2803.6122	126.07	$\nu_s CH_2$
2777.22	2908.81	2796.2391	39.66	2907.28	2794.7683	38.30	$\nu_s CH_2$
2215.73	2902.29	2789.9714	29.66	2900.69	2788.4333	28.73	$\nu_s CH_2$
1663.09	1707.86	1641.7658	171.49	1699.48	1633.7101	164.81	νCO, ρNH, νCC
1608.55	1654.13	1590.1152	60.64	1650.48	1586.6064	52.53	νCC, ρNH
1564.17	1646.62	1582.8958	28.02	1645.48	1581.7999	32.82	δOH, ρNH
	1611.41	1549.0484	204.35	1606.38	1544.2131	106.64	νCN, ρNH, νCC
	1607.98	1545.7512	131.52	1603.18	1541.1369	245.84	νCN, ρNH, νCC, δOH, νCO
1554.37	1589.83	1528.3036	851.30	1588.72	1527.2365	815.40	ρ CN, δNH
1530.60	1547.25	1487.3714	30.46	1549.22	1489.2652	41.80	νCC, ρCH, ρNH
	1509.84	1451.4092	9.24	1512.50	1453.9663	9.95	δCH_2
	1497.53	1439.5756	1.51	1500.51	1442.4403	1.08	δCH_2
	1492.82	1435.0479	5.81	1492.54	1434.7787	12.86	δCH_2, δCH_3
	1488.08	1430.4913	10.21	1491.54	1433.8174	10.30	δCH_2
	1486.42	1428.8955	6.21	1488.54	1430.9335	6.30	δCH_3
	1483.44	1426.0309	9.09	1486.88	1429.3377	1.81	δCH_2
	1482.83	1425.4445	1.91	1485.68	1428.1842	9.37	δCH_2
	1477.86	1420.6668	1.22	1481.67	1424.3294	1.03	δCH_2
	1441.43	1385.6467	3.03	1443.92	1388.0403	3.11	νCC, ρCH, δCH_3
	1434.23	1375.8414	17.62	1434.21	1378.7061	15.60	ωCH_2
	1417.45	1362.5947	2.86	1417.88	1363.0080	3.54	ωCH_2
	1415.08	1360.3164	1.53	1415.37	1360.5952	0.72	ωCH_2, ωCH_3
	1414.20	1359.4705	0.38	1415.23	1360.4606	1.91	ωCH_2, ωCH_3
1403.32	1405.49	1351.0975	17.65	1405.80	1351.3955	13.54	ωCH_2
1376.48	1387.70	1333.9960	51.73	1387.32	1333.6307	34.12	ωCH_2
1359.97	1379.10	1325.7288	84.80	1375.68	1322.4412	84.98	ρCH, ρNH, νCN, ωCH_2
1309.69	1365.22	1312.3860	6.18	1366.97	1314.0683	4.47	ρCH_2
	1354.97	1302.5327	19.73	1359.05	1306.4548	20.56	νCC, ρCH
	1346.21	1294.1117	39.67	1344.27	1292.2468	49.10	νCC, ρCH, ωCH_2
	1336.61	1284.8832	33.44	1333.79	1282.1723	11.54	$t CH_2$
	1310.00	1259.3030	28.58	1311.25	1260.5046	66.34	$t CH_2$
	1309.02	1258.3609	46.66	1308.31	1257.6784	10.39	$t CH_2$
1261.08	1290.64	1240.6922	400.63	1282.50	1232.8673	234.19	νCC, νCN, ρCH, ωCH_2
1213.71	1261.17	1212.3627	66.47	1260.51	1211.7283	69.09	$t CH_2$
	1236.94	1189.0704	0.74	1235.08	1187.2824	3.81	νCC, ρCH
	1233.57	1185.8308	4.91	1233.62	1185.8789	97.02	ρCH_2
	1222.56	1175.2469	90.78	1221.41	1174.1414	92.80	νCC, ρCH
	1214.06	1167.0759	81.51	1209.98	1163.1538	104.93	νCC, νCN, νCO, ρCH_2, ρCH, ρNH

Table 4. Comparison of the theoretical and experimental vibrational spectra and proposal assignment for compound **II** (*Continued*)

	Calculated IR (km mol^{-1})						
Experimental	B3LYP 6-31G+(2d,p)			B3LYP 6-311G+(2d,p)			
(cm^{-1})	Unscaled	Scaled	IR$_{int}$	Unscaled	Scaled	IR$_{int}$	Assignments(a)
1174.80	1183.63	1137.8235	78.35	1176.93	1131.3828	104.93	νCC, νCN, νCO, ρCH$_2$, ρCH, ρNH
1146.41	1171.09	1125.7688	36.24	1165.74	1120.6259	30.39	νCC, νCN, νCO, ρCH$_{2,}$ ρNH
	1153.23	1108.6000	23.53	1151.20	1106.6486	20.48	νCC, νCN, νCO, ρCH$_2$, ρCH
	1150.16	1105.6488	30.58	1150.57	1106.0429	39.43	νCC, ρCH
1117.69	1133.86	1089.9796	107.58	1130.20	1086.4613	97.08	νCC, νCN, νCO, δCH$_2$
1079.85	1123.52	1080.0398	26.28	1121.57	1078.1652	38.21	νCC, νCN, νCO, ρCH$_2$
1041.91	1100.23	1057.6511	23.57	1095.57	1053.1714	28.64	νCC, νCN, νCO, ρNH.
	1092.57	1050.2875	7.09	1091.91	1049.6531	6.92	ρCH$_2$
1015.62	1082.62	1040.7226	36.97	1080.25	1039.4056	41.00	νCC, νCN, νCS, ρNH
	1065.87	1024.6208	9.66	1063.42	1022.2656	10.51	νCC, νCN, νCS, ρNH
1004.05	1062.96	1021.8234	10.40	1063.33	1022.1791	15.67	tCH$_3$
	1049.82	1009.1920	5.52	1047.83	1007.2790	7.43	νCC, νCN, νCO, ωCH$_2$
	1034.70	994.65711	11.01	1039.67	999.43477	9.70	νCC, ρCH$_2$, ρCH$_3$
	1013.34	974.12374	24.68	1032.50	992.54225	7.88	νCC, νCN, νCO, ωCH$_2$
	1008.24	969.22111	0.66	1009.61	970.53809	4.96	ωCH$_3$
	996.24	957.68551	0.78	996.79	958.21423	0.85	tCH
968.95	987.97	949.73556	1.32	988.58	950.32195	1.01	tCH
916.47	925.60	889.77928	12.73	924.77	888.98140	11.84	νCC, νCN, νCO, ωCH$_2$
881.43	905.96	870.89935	13.85	906.45	871.37039	11.02	νCC, νCN, νCO
861.68	882.88	848.71254	42.80	882.41	848.26073	41.85	νCC, νCN, νCO, tCH$_2$
841.74	867.47	833.89891	6.21	867.98	834.38917	7.07	νCC, νCN, νCO, tCH$_2$
810.03	860.47	827.16981	2.82	860.34	827.04484	5.14	νCC, νCN, νCO, ρCH$_2$
	859.04	825.79515	9.61	856.05	822.92087	9.30	ωCH$_,$ ωNH, tCH$_3$
	819.04	787.34315	2.26	820.19	788.44865	2.39	νCC, νCN, νCS
	804.08	772.96210	5.08	800.35	769.37646	3.84	νCC, νCN, νCO, ωNH
	799.59	768.64587	5.10	795.03	764.26234	7.30	ωNH
794.59	775.07	745.07479	118.09	771.58	741.71985	118.10	ωNH
756.76	761.07	731.61659	15.37	762.28	732.77976	14.91	νCS, ρCH$_2$
714.17	754.91	725.69498	23.46	751.58	722.49385	19.34	ωNH
	749.40	720.39822	17.87	749.35	720.35016	27.65	νCS, νCC, ρCH$_2$
684.66	705.03	677.74534	3.33	703.19	675.97655	3.38	νCC, ωNH
629.19	664.81	639.08185	232.11	660.88	635.30394	221.83	ωOH
618.68	650.36	625.19107	0.50	654.68	629.34388	1.73	νCC
	642.30	617.44299	14.68	643.30	618.40429	17.68	ωCS, ωNH
	632.65	608.16645	4.12	633.69	609.16620	4.50	ρCH$_2$
591.01	617.78	593.87191	28.16	618.24	594.31411	28.22	νCC, νCS, ρCH$_2$
	582.45	559.90919	2.02	582.12	559.59196	1.87	νCC, ωCS, ρCH$_2$
	523.37	503.11558	6.43	522.98	502.74067	6.10	νCC, ωCS, ωCH$_2$
	501.48	482.07272	1.10	500.91	481.52478	0.85	νCC, νCO, νCN, ωCH$_2$
	494.70	475.55511	0.81	495.55	476.37222	0.68	νCC, νCO, νCN
476.73	485.70	466.90341	5.15	482.95	464.25984	5.67	*tCC,*νCC, νCO, νCN
449.76	448.62	431.25841	3.96	449.09	431.71022	4.01	νCC, νCO, νCN
	421.37	405.06298	0.37	421.10	404.80343	0.44	*tCC,*
	415.38	399.30479	0.06	415.20	399.13176	0.16	ρCO, ρCC
	387.01	372.03271	9.91	388.81	373.76305	9.89	ρCO, ρCC
	357.16	343.33791	15.26	358.76	344.87599	26.40	ρCO, ρCC
	347.91	334.44588	56.94	355.46	341.70370	44.96	ρOH
	336.91	323.87158	10.10	336.37	323.35248	9.80	ρCH$_2$
	328.68	315.96008	7.62	328.30	315.59479	7.68	ρCH$_2$
	308.95	296.99364	9.42	308.84	296.88789	9.84	ρCH$_{2,}$ ρCH$_3$
	288.68	277.50808	4.11	286.30	275.22019	4.10	tOH
	277.30	266.56849	97.85	276.25	265.55913	99.88	ρCN, ρCC
	262.23	252.08170	3.03	262.11	251.96634	2.97	ρCH$_2$
	256.31	246.39080	0.37	256.53	246.60229	0.25	ρCN, ρCS
	254.11	244.27594	7.27	254.92	245.05460	7.82	ρCC, ρCS, ρOH
	208.27	200.20995	1.35	207.81	199.76775	1.57	ρCH$_2$
	166.13	159.70077	1.81	168.22	161.70989	2.87	Skeletal vibration
	162.29	156.00938	8.38	163.13	156.81687	6.65	Skeletal vibration
	154.53	148.54969	3.90	152.67	146.76167	3.76	Skeletal vibration
	129.56	124.54603	4.77	131.76	126.66089	5.34	Skeletal vibration

Table 4. Comparison of the theoretical and experimental vibrational spectra and proposal assignment for compound **II** (*Continued*)

Experimental	Calculated IR (km mol^{-1})						
	B3LYP 6-31G+(2d,p)			B3LYP 6-311G+(2d,p)			
(cm^{-1})	Unscaled	Scaled	IR$_{int}$	Unscaled	Scaled	IR$_{int}$	Assignments$^{(a)}$
	115.57	111.09744	2.00	114.82	110.37647	0.90	Skeletal vibration
	111.18	106.87733	0.52	111.57	107.25224	1.57	Skeletal vibration
	104.39	100.35011	0.76	102.78	98.802414	0.71	Skeletal vibration
	87.61	84.219493	1.26	88.35	84.930855	1.15	Skeletal vibration
	64.05	61.571265	0.56	64.19	61.705847	0.58	Skeletal vibration
	52.76	50.718188	2.33	51.79	49.785727	2.45	Skeletal vibration
	19.27	18.524251	0.08	25.28	24.301664	0.13	ρCH_3
	15.03	14.448339	0.32	14.96	14.381048	0.20	Skeletal vibration

[a] Vibrational assignment: ν, stretching; δ, scissoring; ω, wagging; ρ, rocking; t, twisting.

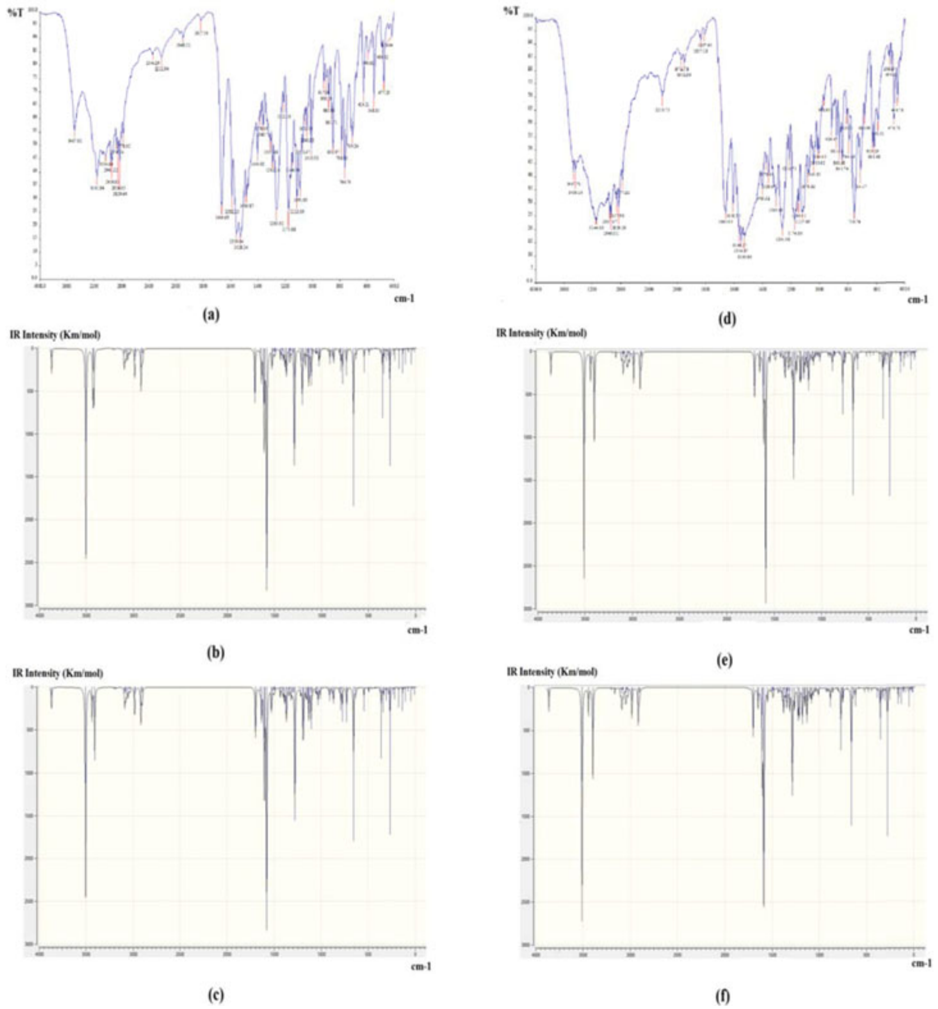

Figure 7. The IR spectrum of Compound **I**: (a) Experimental; (b) B3LYP/6-31G +(2d,p); (c) B3LYP/6-311G +(2d,p) and Compound **II**: (d) Experimental; (e) B3LYP/6-31G+(2d,p); (f) B3LYP/6-311G +(2d,p).

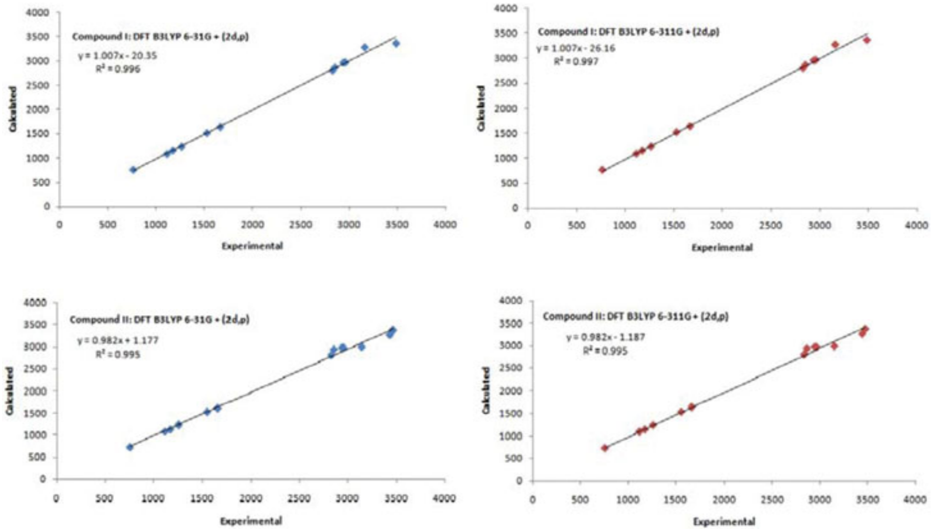

Figure 8. The linear corrected between the calculation and FT-IR spectrum of compound **I** and **II**.

provide different values of correlation coefficient, where a good linearity between the calculated and experimental frequencies were obtained from higher basis sets. As can be seen from the correlation graphic [Fig. 8], obtained correlations were 0.996 and 0.997 for compound **I** and 0.995 for compound **II**. The use of higher extended basis set has correlated the experimental and theoretical data well.

2.3. NMR Analysis

Both compounds were characterized by using ^{1}H and ^{13}C NMR. The ^{1}H 400.11 MHz and ^{13}C 100.61 MHz NMR spectra were recorded in solvent of $CDCl_3$ at room temperature by Bruker Avance III 400 Spectrometer. Theoretically, the compounds were calculated by using DFT method with basis sets of B3LYP/6-31G+(2d,p) and B3LYP/6-311G+(2d,p). The results of the calculated values shifted to higher values of chemical shift and further corrected with the TMS isotropic chemical shift values. All the experimental and calculated results are tabulated in Table 5. As can be seen from the table, the experimental and theoretical values were in a good agreement where the values had the same range of chemical shift.

In ^{1}H NMR, the NH resonance can be clearly seen where two single peaks were observed at the most downfield area (10.867 and 8.977 ppm in compound **I** and 10.947 and 9.010 ppm in compound **II**). Meanwhile, the calculated chemical shifts showed higher values for about 1 to 2 ppm differences but the use of basis set B3LYP/6-311G+(2d,p) gave a better agreement with the experimental results. The high shifted values were due to the presence of strong intra and intermolecular N—H . . . O hydrogen bonds in the molecules. The hydrogen atoms of the aromatic ring, morpholine ring, and the methylene group were generally in the same range as the previously reported studies [3,9,33,36]. These results were also confirmed by the calculated values, where the values did not deviate higher than the experimental results (Table 5). The presence of the methyl group in compound **II** gave single peaks at δ values of 2.455 ppm and the values of the calculated chemical shift of methyl group were also in same range of 2.0856–2.7125 ppm for B3LYP/6-31G+(2d,p)

Table 5. The experimental and calculated NMR chemical shift of compounds **I** and **II**

	Compound **I**			Compound **II**		
Chemical Shift, δ (ppm)[a]	Experimental	B3LYP 6-31G + (2d,p)[b]	B3LYP 6-311G + (2d,p)[c]	Experimental	B3LYP 6-31G + (2d,p)[b]	B3LYP 6-311G + (2d,p)[c]
^{1}H NMR						
N1–H1N1	10.867	11.3438	11.0203	10.947	11.2099	11.0196
N2–H1N2	8.977	11.2097	10.9460	9.010	11.7561	11.4272
Aromatic Proton	7.816, 7.518	8.7768, 8.3515, 7.6150, 7.5960.	8.9947, 8.5393, 7.7711, 7.6654.	7.758, 7.328	8.6511, 8.5817, 7.4506, 7.3907	8.6804, 8.5982, 7.5257, 7.4027.
Proton of Morpholine moiety	3.775, 2.494,	3.7561, 3.7247, 3.6701, 3.6114, 2.6598, 2.3614, 2.2896, 1.9317.	3.8083, 3.7728, 3.7501, 3.7220, 2.7800, 2.4526, 2.4157, 2.0030.	3.771, 2.488	3.7220, 3.6799, 3.6253, 3.5612, 2.6621, 2.3000, 2.2626, 1.9335.	3.7225, 3.6723, 3.6226, 3.5330, 2.7090, 2.4193, 2.3713, 2.0912.
Methylene	3.827, 1.916, 1.710	3.4277, 3.3609, 2.3538, 2.1948, 2.0308, 1.7763.	3.5353, 3.3432, 2.5210, 2.2601, 2.0410, 1.8194.	3.823, 1.916, 1.765	4.1952, 2.9423, 2.3863, 2.1838, 2.1082, 1.3327.	4.1442, 2.9224, 2.4193, 2.3625, 2.2082, 2.1677.
Methyl group				2.455	2.7125, 2.4085, 2.0856.	2.7475, 2.3868, 2.1680.
^{13}C NMR						
C8	179.39	179.503	189.981	179.72	179.382	191.037
C9	165.30	164.159	171.521	166.40	163.744	172.188
C3	140.12	145.292	154.291	144.53	140.674	150.231
C6	130.23	127.265	134.735	129.81	126.806	133.494
C1 & C5	129.50	129.309, 126.611	136.519, 133.689	128.95	127.614, 125.277	135.879, 132.694
C2 & C4	128.84	126.133, 125.561	133.154, 132.515	127.47	126.577, 126.431	133.165, 132.319
C14 & C13	66.79	68.8281, 68.4852	70.307, 70.1251	66.81	69.0633, 68.8558	70.2985, 70.1022
C15 & C12	53.85	57.7378, 54.0620	58.573, 54.7693	53.82	57.6925, 52.8373	58.6170, 54.735
C11	56.76	58.6090	60.1520	56.69	58.1384	59.4288
C9	44.94	46.7859	47.0636	44.72	45.1407	45.0386
C10	24.60	30.3144	29.3706	24.72	29.7854	29.6148
C16				21.65	25.5784	22.6210

[a] The atoms numbering are referred to the X-ray molecular diagram in Fig. 1.

[b] The isotropic chemical shift with respect to Tetramethysilane (TMS) in B3LYP 6-31G + (2d,p) are 31.6143 ppm for ^{1}H NMR and 191.2113 ppm for ^{13}C NMR.

[b] The isotropic chemical shift with respect to Tetramethysilane (TMS) in B3LYP 6-311G + (2d,p) are 31.8821 ppm for ^{1}H NMR and 182.4656 ppm for ^{13}C NMR.

and 2.7475–2.1680 ppm for B3LYP/6-311G+(2d,p). In addition, the different substituent atom or group did not affect the values of the chemical shift.

In ^{13}CNMR, the highest δ values were from the thione (C = S) and carbonyl groups (C = O). These groups were at the most deshielded area compared to other carbon atoms because of the environmental factor and the increase of electronegativity from sulphur and oxygen atoms. Aydin et al. [9] in their report stated that the carbon atoms of thiocarbonyl showed that the highest value (180.41 ppm) was due to the lower excitation energy n–π^* and the possibility of a very strong electron-withdrawing neighbors reduced the nucleophilic character of the thione group. From Table 5, δ values of thione group and carbonyl group were 179.39 ($\delta_{C=S}$) and 165.30 ($\delta_{C=O}$) ppm (compound **I**) and 179.72 ($\delta_{C\,=\,S}$) and 166.40 ($\delta_{C\,=\,O}$) ppm (compound **II**), whereas theoretical values gave higher values of C = S and C = O chemical shift from B3LYP/6-311G+(2d,p) basis set where the difference was almost 10 to 11 ppm. Meanwhile, the B3LYP/6-31G+(2d,p) showed a very good agreement with the experimental values. Other carbon atoms were located in the same range as the previously reported structures [3,9,33,36] and calculated δ values were in a good agreement with the experimental results especially from the B3LYP 6-31G+(2d,p) basis set.

As seen from Table 5, the results of the ^{1}H and ^{13}C NMR calculated from two different basis sets were not systematic in relation with the experimental results and it was difficult to decide which basis sets showed the best agreement with the experimental values. Even though in the same basis set, there were some values in a very good agreement and there were some that showed big differences with experimental values.

3. Experimental

3.1. Physical Measurement

Infrared spectra of the compounds were recorded from KBr discs in the spectral range of 400–4000 cm^{-1} by using FTIR Pelkin-Elmer System 100 Spectrometer. The ^{1}H NMR (400.11 MHz) and ^{13}C NMR (100.61 MHz) spectra were recorded on Bruker Avance III 400 Spectrometer in solution of deuterated chloroform (CDCl$_3$) as solvents at room temperature in the range of 0–15 ppm and 0–200 ppm. The chemical shifts were also referenced to the trimethylsilyl (TMS) as internal standard.

3.2. Synthesis

The reaction process of compounds **I** and **II** is shown in Scheme 1. The reactions were done under ambient temperature. All the chemicals used were purchased from suppliers and used without further purifications.

*3.2.1. Compound **I**.* A solution of 4-chlorobenzoyl chloride (1.0 g, 6 mmol) was added dropwise to ammonium thiocyanate in acetone (50 ml). The resulting solution was refluxed with constant stirring for 1 h. The product was cooled down at room temperature and 3-morpholinopropyl amine (1.0 g, 6 mmol) in 50 ml acetone was added dropwise. The solution mixture was refluxed with stirring for 4 h. The solution was filtered and the solution was poured into ice. The solid product was recrystallized to obtain yellow crystal product (1.21g, 59%). FT-IR (KBr, cm^{-1}): 3487.61 (ν_{OH}), 3161.84 (ν_{NH}), 2961.22, 2939.85, 2854.63, 2829.49 (ν_{CH}, ν_{CH2}), 1666.63 ($\nu_{C=O}$), 1528.24, 1265.92, 1175.88 (ν_{CN}), 764.76 ($\nu_{C=S}$). ^{1}H NMR (CDCl$_3$; δ, ppm): 10.867, 8.977 (2 × s, 1H, NH), 7.816 (d, J = 3.4 Hz, 2H, Ar), 7.518 (d, J = 2.4 Hz, 2H, Ar), 3.775 (t, J = 4.8 Hz, 4H, proton of morpholine

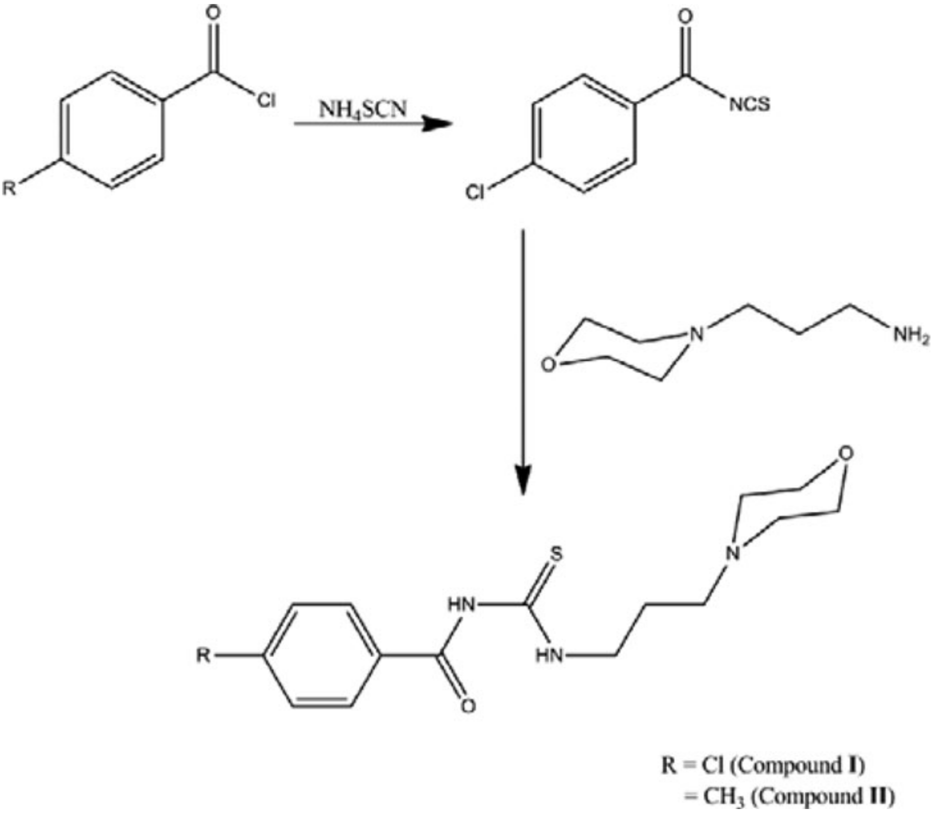

Scheme 1. The reaction process for compound I and II.

ring), 2.494 (t, $J = 6.6$ Hz, 4H, proton of morpholine ring), 3.827 (q, $J = 18.8$ Hz, 2H, CH_2), 1.916 (t, $J = 6.8$ Hz, 2H, CH_2), 1.710 (m, 2H, CH_2). ^{13}C NMR ($CDCl_3$; δ, ppm): 179.39 (C = S), 165.30 (C = O), 140.12, 130.23, 129.50, 128.84 (aromatic ring), 66.79, 53.85 (morpholine ring), 56.85, 44.94, 24.60 (methylene).

*3.2.2. Compound **II**.* Compound **II** was synthesized with a similar procedure as described in compound **I** but solution of 4-methylbenzoyl chloride (1.0 g, 6 mmol) was used. Colourless crystals were obtained (1.19 g, 62%). FT-IR (KBr, cm^{-1}): 3467.70 (ν_{OH}), 3436.19, 3144.83 (ν_{NH}), 2957.67, 2940.02, 2857.98, 2829.28 (ν_{CH}, ν_{CH2}), 1663.09 ($\nu_{C=O}$), 1554.37, 1261.08, 1174.80 (ν_{CN}), 756.76 ($\nu_{C=S}$). ^{1}H NMR ($CDCl_3$; δ, ppm): 10.947, 9.010 (2 × *s*, 1H, NH), 7.758 (d, J=8.4 Hz, 2H, Ar), 7.328 (d, $J = 8$ Hz, 2H, Ar), 3.771 (t, $J = 4.8$ Hz, 4H, proton of morpholine ring), 2.488 (t, $J = 6.4$ Hz, 4H, proton of morpholine ring), 3.823 (q, $J = 18$ Hz, 2H, CH_2), 1.916 (t, $J = 6.8$ Hz, 2H, CH_2), 1.765 (m, 2H, CH_2), 2.455 (s, 3H, methyl). ^{13}C NMR ($CDCl_3$; δ, ppm): 179.72 (C=S), 166.40 (C=O), 144.53, 129.81, 128.95, 127.47 (aromatic ring), 66.81, 53.82 (morpholine ring), 56.69, 44.72, 24.72 (methylene), 21.65 (methyl).

Table 6. Crystallographic data for compound **I** and **II**

Compound	I	II
CCDC deposition numbers	944766	944767
Molecular formula	$C_{15}H_{20}ClN_3O_2S.H_2O$	$C_{16}H_{23}N_3O_2S.H_2O$
Molecular weight	359.87	339.45
Crystal system	Monoclinic	Triclinic
Space group	*C*2/*c*	*P*-1
a/Å	16.4318	9.3319(3)
b/Å	13.0017	9.6187(3)
c/Å	16.2908	10.3072(3)
α /°	90.000	112.734(1)
β/°	97.394	90.143(2)
γ/°	90.000	93.455(2)
V/ Å^3	3451.45(5)	851.42(5)
Z	8	2
D_{calc} (g cm^{-3})	1.385	1.324
Crystal Dimensions (mm)	0.35 × 0.29 × 0.19	0.28 × 0.17 × 0.15
μ/mm^{-1}	0.36	0.21
Radiation λ (Å)	0.71073	0.71073
$T_{\text{min}}/T_{\text{max}}$	0.884/0.936	0.944/0.969
Reflections measured	26263	4887
Ranges/indices (h, k, l)	$23 \leq h \leq 22$; $18 \leq k \leq 18$; $23 \leq l \leq 18$.	$13 \leq h \leq 13$; $13 \leq k \leq 12$; $24 \leq l \leq 14$.
θ limit (°)	2.0–30.2	2.1–30.0
Unique reflections	5105	4887
Observed reflections ($I > 2\sigma(I)$)	4342	4031
Parameters	218	226
Goodness of fit on F^2	1.04	1.06
R_1, wR_2 [$I \geq 2\sigma(I)$]	0.040, 0.096	0.047, 0.134
Largest diff. peak and hole, e/Å^{-3}	0.60 and -0.58	0.45 and -0.29

3.3. *X-Ray Crystallography Studies*

The single crystal of compounds **I** and **II** was mounted on the glass fiber. The crystal structures were determined by single crystal X-ray diffraction from data collected at low temperature (100K) using the Oxford Cryosystem Cobra low-temperature attachment [45]. The data were collected using a Bruker APEX2 CCD diffractometer with the graphite monochromated MoKα ($\lambda = 0.71073$ Å) radiation and with APEX2 software [46]. The collected data were reduced using SAINT program [46]. The empirical absorption corrections were performed by the SADABS program [46]. The structure was solved by direct methods and refined by full matrix least-squares using the SHELXTL software package [47]. The nonhydrogen atoms were refined anisotropically. The hydrogen atoms which bounded to the nitrogen atom and the oxygen of the water molecule were found from the difference fourier maps and refined freely. All the other hydrogen atoms were positioned geometrically and refined using riding model. A rotating group model was applied to the methyl group of compound **II**. Besides, the studied structure of compound **II** was an inversion twin with a domain ratio of 0.81387 (22): 0.18613 (22). In the final refinement, the same U^{ij} parameter (EADP constraint) was used to the atom pair S1 and C8 of compound **I** and ten outliers (−1 −1 2, 7 −2 4, 8 0 1, 5 0 1, −4 0 1, −1 0 1, −5 −2 4, 0 0 1, −1 −2 4, and 6 −2 4) were omitted from compound **II**. The structure analysis and presentation of the results were made using PLATON [47]. Table 6 shows the main crystal data and structure refinement for compounds **I** and **II**.

3.4. Computational Calculation

The molecular geometries were optimized to standard convergence criteria and harmonic frequencies calculated by using DFT hybrid method with Becke's nonlocal three parameter exchange and the Lee, Young and Parr correction (B3LYP) using the 6-31G+(2d,p) and 6-311G+(2d,p) basis sets as implemented in the GAUSSIAN 09 program package [49]. The optimized structural parameters were used to calculate the vibrational wavenumbers and isotropic chemical shifts. The calculated vibrational frequencies corresponded to potential energy minima in which no imaginary frequency was found. The gauge-invariant atomic orbital (GIAO) method was used to calculate the ^{1}H and ^{13}C NMR chemical shifts in ppm relative to TMS as internal standard. The GIAO approach allows the computation of the absolute chemical shielding due to the electronic environment of the individual nuclei and this method is often more accurate than those calculated with other approaches for the same basis set [1]. Gauss View molecular visualization program has been used for the animation of vibrational band assignments and preparation of the spectrum [50].

4. Conclusion

The crystal structure of compounds **I** and **II** were successfully synthesized and characterized by X-Ray Crystallography analysis, FT-IR, and NMR spectroscopy. In the crystal, the main molecules with the water molecules were connected into a centrosymmetry dimer in compound **I**, whereas in compound **II**, the molecules were linked into one-dimensional column. The C—H . . . π interactions were also observed in both molecules. The ground state geometries of the structure were optimized using DFT/B3LYP6-31G+(2d,p) and DFT/B3LYP6-311G+(2d,p) basis sets and further used to calculate the vibrational frequencies and the isotropic chemical shift. All the calculated values were in a good agreement with the experimental results. The calculated values from the DFT/B3LYP6-311G+(2d,p) basis set gave better agreement as compared to the DFT/B3LYP6-31G+(2d,p) basis set. The observed intermolecular interactions in the crystal packing are the main cause of the torsion angles differences where these interactions are not taken into consideration during the optimization process. The differences are also observed in the calculated molecular vibrations and chemical shifts. In theoretical FTIR and NMR analysis, the atoms involved in the intermolecular hydrogen bond show a significant difference in the wavenumber and chemical shift values, respectively, compared with the observed data. The correlation values of 0.995, 0.996, and 0.997 were obtained from the vibrational frequency studies. We hope that the proposed results can assist others in the experimental and theoretical studies that are related to the title compounds **I** and **II**, where both compounds have been calculated in the presence of water molecules.

Supplementary Material

Crystallographic data (excluding the structure factors file) have been deposited with the Cambridge Crystallographic Data Centre, 12 Union Road, Cambridge CB221EZ, UK (fax: +44-1223-336033; email: deposit@ccdc.cam.ac.uk or http://www.ccdc.cam.ac.uk) as supplementary publication no. CCDC 944766 for compound **I** and 944767 for compound **II**.

Acknowledgments

The authors thank the Malaysian Government and Universiti Sains Malaysia (USM) for the research facilities and USM Short Term Grant, No. 304/PFIZIK/6312078 and FRGS Grant 59178 to conduct this work. SA thanks the Malaysian government and USM for the Academic Staff Training Scheme Fellowship (ASTS).

References

[1] Atiş, M., Karipchi, F., Sariboğa, B., Taş, M., & Çelik, H. (2012). *Spectrochim. Acta A*, *98*, 290.
[2] Arslan, H., Mansuroglu, D. S., VanDerveer, D., & Binzet, G. (2009). *Spectrochim. Acta A*, *72*, 561.
[3] Arslan, N.B., Kazak, C., & Aydin, F. (2012). *Spectrochim. Acta A*, *89*, 30.
[4] Arslan, H., Külcü, N., & Flörke, U. (2006). *Spectrochim. Acta A*, *64*, 1065.
[5] Estévez-Hernández, O., Otazo-Sánchez, E., Hidalgo-Hidalgo de Cisneros, J. L., Naranjo-Rodríguez, I., & Ruguera, E. (2005). *Spectrochim. Acta A*, *62*, 964.
[6] Yang, W., Zhu, W., Zhou, W., Liu, H., & Fan, J. (2012). *J. Flourine Chem.*, *144*, 38.
[7] Saeed, A., Erben, M. F., Shaheen, U., & Flörke, U. (2011). *J. Mol. Struct.*, *1000*, 49.
[8] Zhu, W., Yang, W., Zhou, W., Liu, H., Wei, S., & Jianfen, F. (2001). *J. Mol. Struct.*, *1004*, 74.
[9] Aydin, F., Aykaç, D., Ünver, H., & İskeleli, N. O. J. (2012). *Chem. Crystallogr.*, *42*, 381.
[10] Arslan, H., Külcü, N., & Flörke, U. (2006). *Spectrochim. Acta A*, *64*, 1065.
[11] Loto, R. T., Loto, C. A., & Popoola, A. P. I. (2012). *J. Mater. Environ. Sci.*, *3*, 885.
[12] Yaro, A. S., & Abdulaaima, D. A. (2012). *Iraqi J. Chem. Petroleum Eng.*, *13*, 1.
[13] Shetty, S. D., Shetty, P., & Sudhaker Nayak, H. V. (2006). *J. Serb. Chem, Soc.*, *71*, 1073.
[14] Tripathi, R., Chaturvedi, A., & Upadhayay, R. K. (2012). *Res. J. Chem. Sci.*, *2*, 18.
[15] Anitha, S., Sreenivasan, E., & Puroshothaman, S. M. (2004). *J. Trop. Agric.*, *42*, 53.
[16] Anitha, S., Puroshothaman, S. M., & Sreenivasan, E. (2006). *Legume Res.*, *29*, 146.
[17] Saeed, S., Rashid, N., Ali, M., Hussain, R., & Jones, P. (2010). *Eur. J. Chem.*, *1*, 221.
[18] El-Hamdouni, N., Companyó, X., Rios, R., & Moyano, A. (2010). *Chem. Eur. J.*, *16*, 1142.
[19] Takemoto, Y. (2010). *Chem. Pharm. Bull.*, *58*, 593.
[20] Okino, T., Hoashi, Y., Furukawa, T., Xu, X., & Takemoto, Y. (2005). *J. Am. Chem. Soc.*, *127*, 119.
[21] Mohamed, M. S., Kamel, M. M., Kassem, E. M. M., Abotaleb, N., Abd El-moez, S. I., & Ahmed, M. F. (2010). *Eur. J. Med. Chem.*, *45*, 3311.
[22] Marverti, G., Cusumano, M., Ligabue, A., Di Pietro, M. L., Vainiglia, P. A., Ferrari, A., Bergomi, M., Moruzzi, M. S., & Frassineti, C. (2008). *J. Inorg. Biochem.*, *102*, 699.
[23] Keche, A. P., Hatnapure, G. D., Tale, R. H., Rodge, A. H., Birajdar, S. S., & Kamble, V. M. (2010). *Bioorg. Med. Chem Lett.*, *22*, 3445.
[24] Sriram, D., Yogeeswari, P., & Madhu, K. (2006). *Bioorg. Med. Chem Lett.*, *16*, 876.
[25] D'Cruz, O. J., Dong, Y., & Uckun, F. M. (2003). *Biochem. Bioph. Res. Co.*, *302*, 253.
[26] Foresman, J. B., & Frisch, Æ. (1996). *Exploring Chemistry with Electronic Structure Methods*, Gaussian, Inc.: Pittsburgh, PA.
[27] Arslan, H., Flörke, U., & Külcü, N. (2007). *Spectrochim. Acta A*, *67*, 936.
[28] Arslan, H., Flörke, U., Külcü, N., & Binzet, G. (2007). *Spectrochim. Acta A*, *68*, 1347.

[29] Yusof, M. S. M., Mutalib, S. F. A., Arshad, S., & Razak, I. A. (2012). *Acta Cryst. E*, *68*, o982

[30] Yusof, M. S. M., Embong, N. F., Arshad, S., & Razak, I. A. (2012). *Acta Cryst. E*, *68*, o1029.

[31] Yusof, M. S. M., Embong, N. F., Arshad, S., & Razak, I. A. (2012). *Acta Cryst. E*, *68*, o1267.

[32] Yusof, M. S. M., Arshad, S., Razak, I. A., & Rahman, A. A. (2012). *Acta Cryst. E*, *68*, o2670.

[33] Duan, X.-E., Wei, X.-H., Tong, H.-B., Bai, S.-D., Zhang, Y.-B., & Liu, D.-S. (2011). *J. Mol. Struct.*, *1005*, 91.

[34] Yusof, M. S. M., Jusoh, R. H., Khairul, W. M., & Yamin, B. M. (2010). *J. Mol. Struct.*, *975*, 280.

[35] Saeed, A., Erben, M. F., Abbas, N., & Flörke, U. (2010). *J. Mol. Struct.*, *984*, 240.

[36] Hritzová, O., Černák, J., Šafař, P., Frőhlichová, Z., & Csőregh, I. (2005). *J. Mol. Struct.*, *743*, 29.

[37] Cremer, D., & Pople, J. A. (1975). *J. Am. Chem. Soc.*, *97*, 1354.

[38] Fun, H.-K., Arshad, S., Samshuddin, S., Narayana, B., & Sarojini, B. K. (2011). *Acta Cryst. E*, *67*, o3372.

[39] Jie, L., Shuchen, P., Li, H., & Yong, W. (2012). *Acta Cryst. E*, *68*, o13.

[40] Devarajegowda, H. C., Kumar, K. M., Seenivasa, S., Arunkashi, H. K., & Kotresh, O. (2013). *Acta Cryst. E*, *69*, o192.

[41] Bernstein, J., Davis, R. E., Shimoni, L., & Chang, N.-L. (1995). *Angew. Chem. Int. Ed. Engl.*, *34*, 1555.

[42] Saeed, A., Erben, M. F., & Bolte, M. (2011). *J. Mol. Struct.*, *985*, 57.

[43] Subashchandrabose, S., Saleem, H., Erdogdu, Y., Rajarajan, G., & Thanikachalam, V. (2011). *Spectrochim. Acta A*, *82*, 260.

[44] Krishnamoorthy, A., Herbert, F. W., Yip, S., Vliet, K. J. V., & Yildiz, B. (2013). *J. Phys.: Condens. Matter.*, *25*, 045004.

[45] Cosier J., & Glazer A. M. (1986). *J. Appl. Cryst.*, *19*, 105.

[46] Bruker. *SADABS, APEX2 and SAINT*. (2009). Bruker AXS, Inc.: Madison, Wisconsin, USA.

[47] Sheldrick, G. M. (2008). *Acta Cryst. A*, *64*, 112.

[48] Spek, A. L. (2009). *Acta Cryst. D*, *65*, 148.

[49] Frisch, M. J., Trucks, G. W., Schlegel, H. B., Scuseria, G. E., Robb, M. A., Cheeseman, J. R., & Scalmani, G., *et al. Gaussian 09, Revision A.1*, Gaussian, Inc.: Wallingford, CT.

[50] Dennington, R., Keith, T., & Millam, J. (2009). *GaussView, Version 5*, Semichem, Inc.: Shawnee Mission, KS.